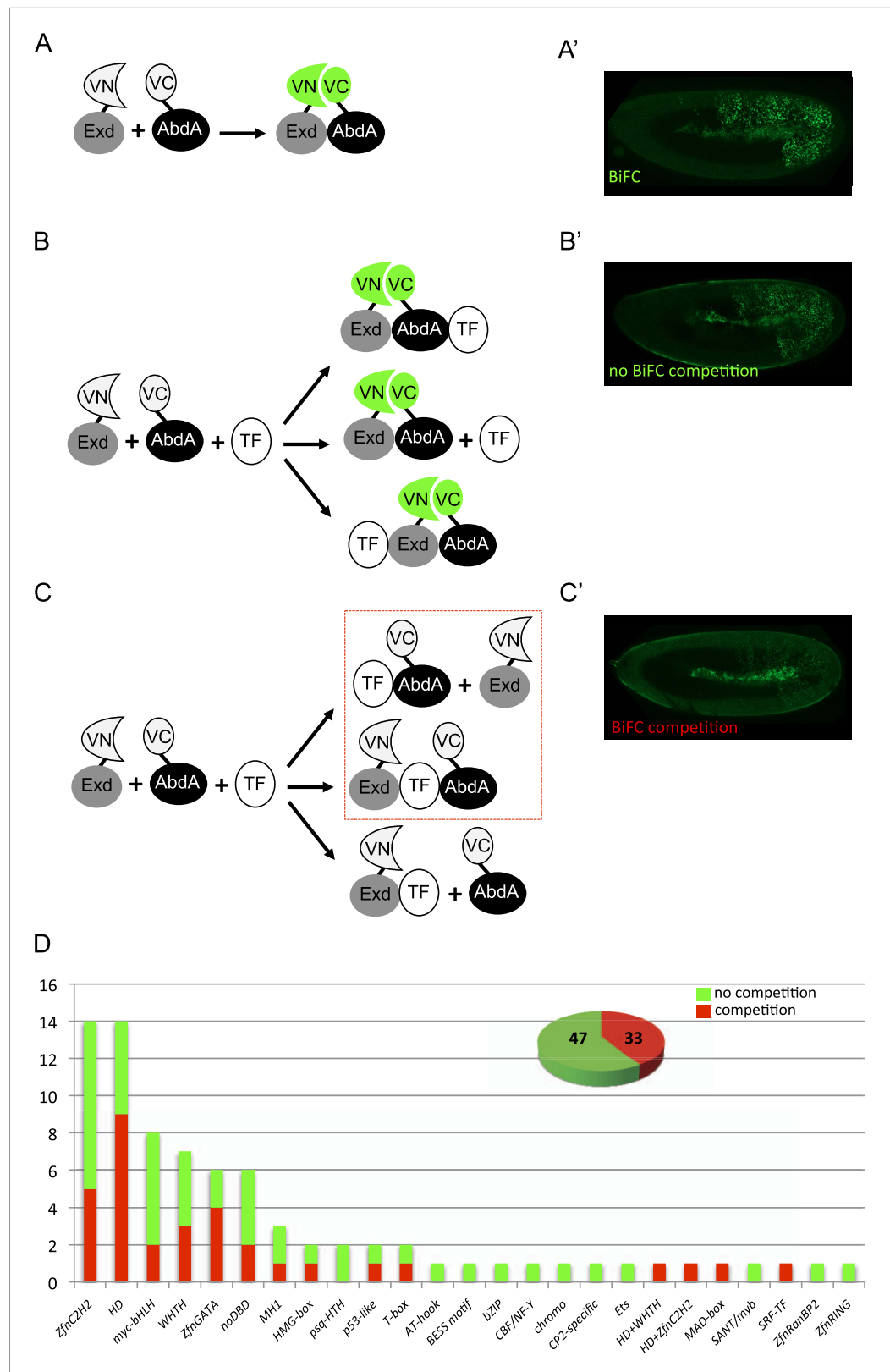# Figures and figure supplements

Inhibitory activities of short linear motifs underlie Hox interactome specificity in vivo

Manon Baëza, et al.

Figure 1. A BiFC competition screen identifies candidate transcription factors (TFs) as potential binding partners of the Hox protein AbdominalA (AbdA). (**A**–**C**) Principle of the competition test. (**A**–**A'**) Co-expression of Extradenticle (Exd) and AbdA proteins fused to the N-(VN) or C-(VC) terminal fragment of the Venus fluorescent protein leads to

Figure 1. continued on next page

Figure 1. Continued

BiFC in the embryo. (**B–B′**) Cases where no BiFC competition could be observed with a cold TF. **B′** is an illustrative picture of non-competitive BiFC resulting from the simultaneous co-expression of the red fluorescent protein RFP (see also *Figure 1—figure supplement 2*). (**C–C′**) Cases where BiFC competition could be observed with a cold TF. **C′** is an illustrative picture of competitive BiFC resulting from the simultaneous co-expression of a nuclear-localized form of Exd (see also *Figure 1—figure supplement 1*). Note that AbdA-interacting partners do not obligatory lead to competitive BiFC. TFs that could be validated in the secondary step as AbdA-binding partners (see *Figure 2*) are indicated (dotted-red box). (**D**) Graph showing the repartition of competitive (red bars) and non-competitive (green bars) TFs with regard to their DNA-binding domain. See also *Supplementary file 1*.
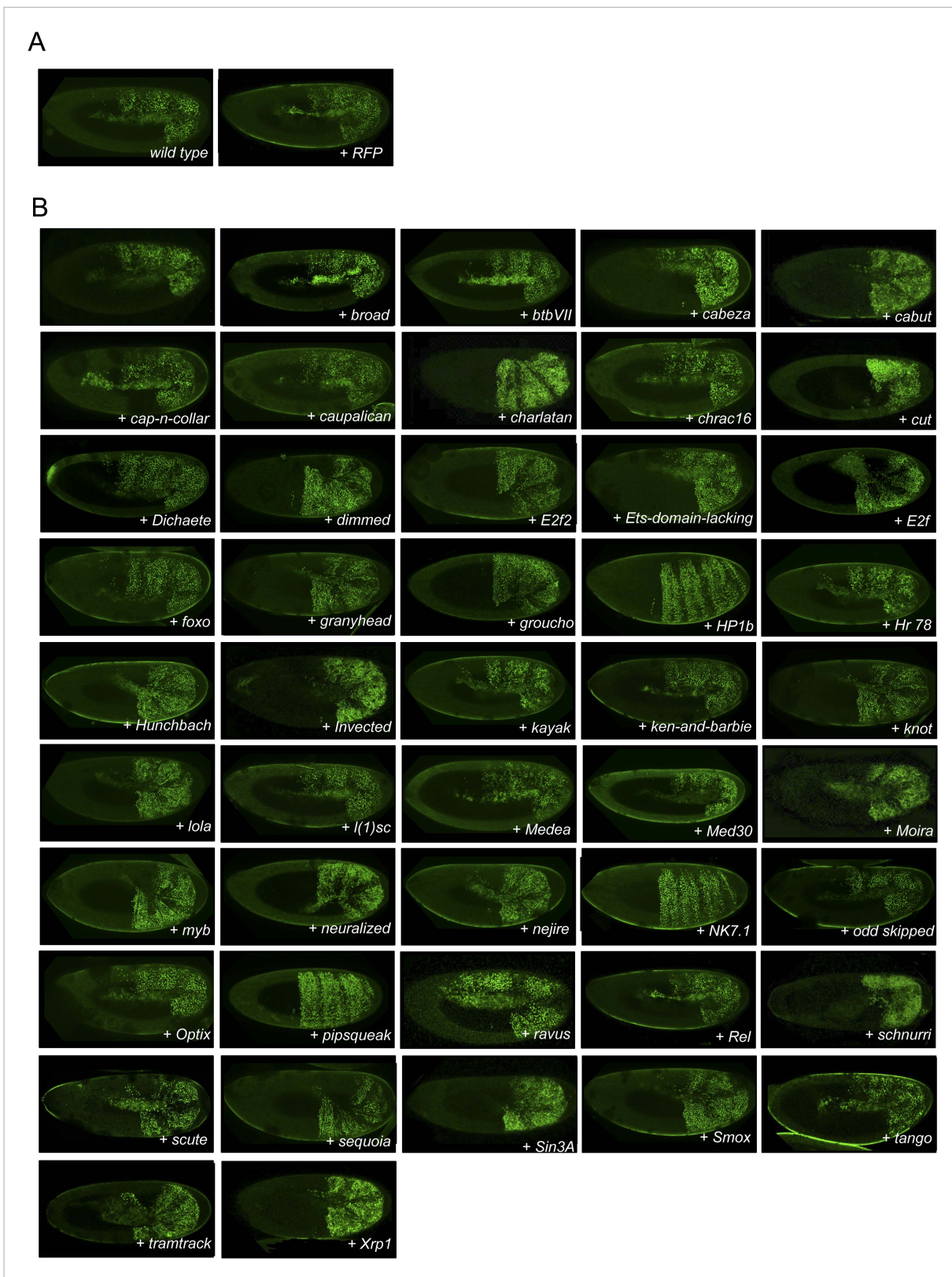DOI: 10.7554/eLife.06034.003
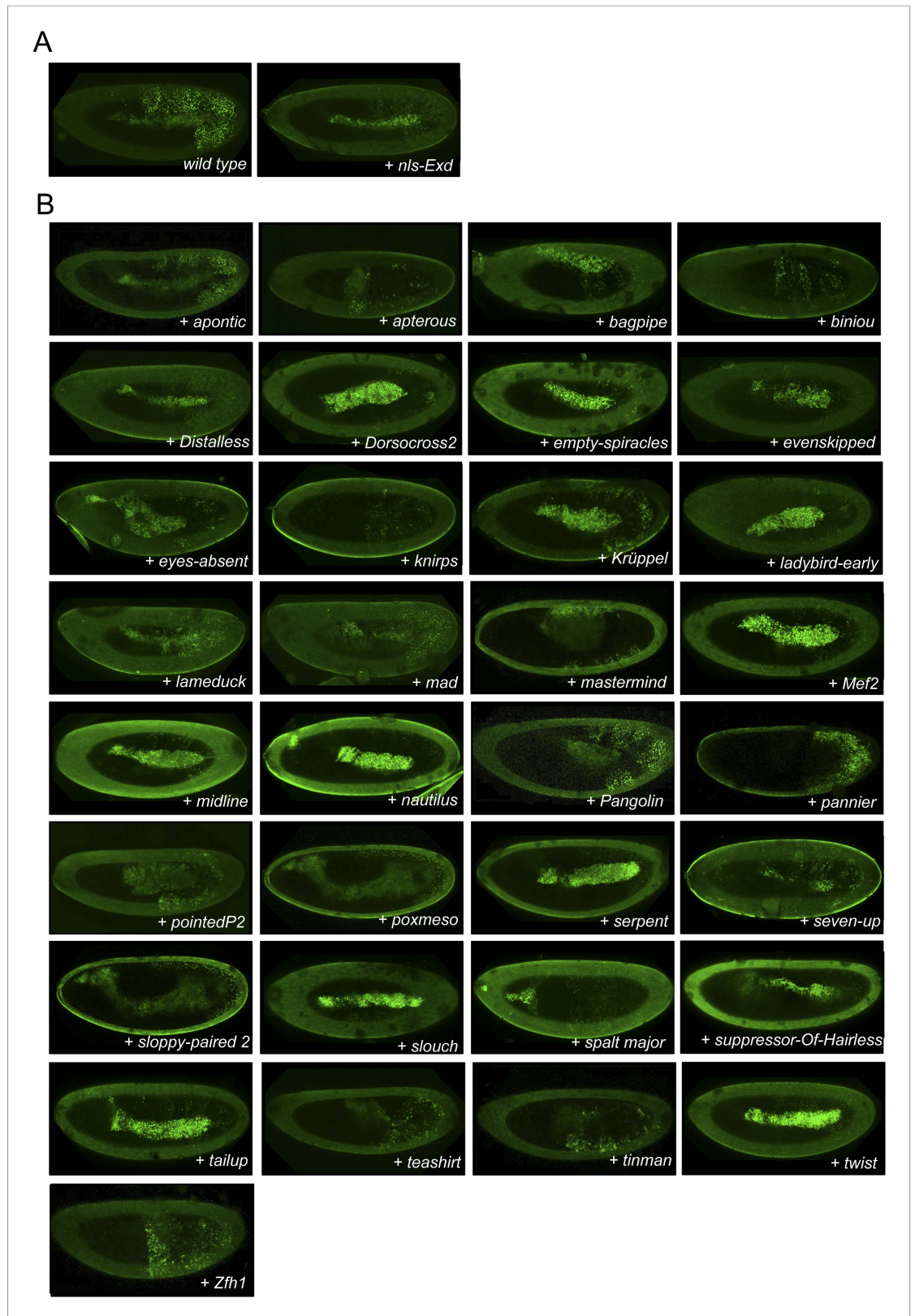
Figure 1—figure supplement 1. Illustrative pictures of competitive TFs. (**A**) Competitive control with the UAS-nls-Exd construct. (**B**) Competitive TFs. Each construct was co-expressed with AbdA and Exd fusion proteins and BiFC

Figure 1—figure supplement 1. continued on next page

Figure 1—figure supplement 1. Continued

was analysed in the epidermis of stage 10–12 of live embryos. The competition was deduced when altered BiFC signals could be observed in the expected or nearly expected proportion of the embryo progeny (see 'Materials and methods').

Figure 1—figure supplement 2. Illustrative pictures of non-competitive TFs. (**A**) Non-competitive control with the UAS-RFP construct. (**B**) Non-competitive TFs. Each construct was co-expressed with AbdA and Exd fusion proteins and BiFC was analysed in the epidermis of stage 10–12 of live

Figure 1—figure supplement 2. continued on next page

Figure 1—figure supplement 2. Continued

embryos. Absence of competition was deduced when no clear altered BiFC signals could be observed in the embryo progeny (see 'Materials and methods').
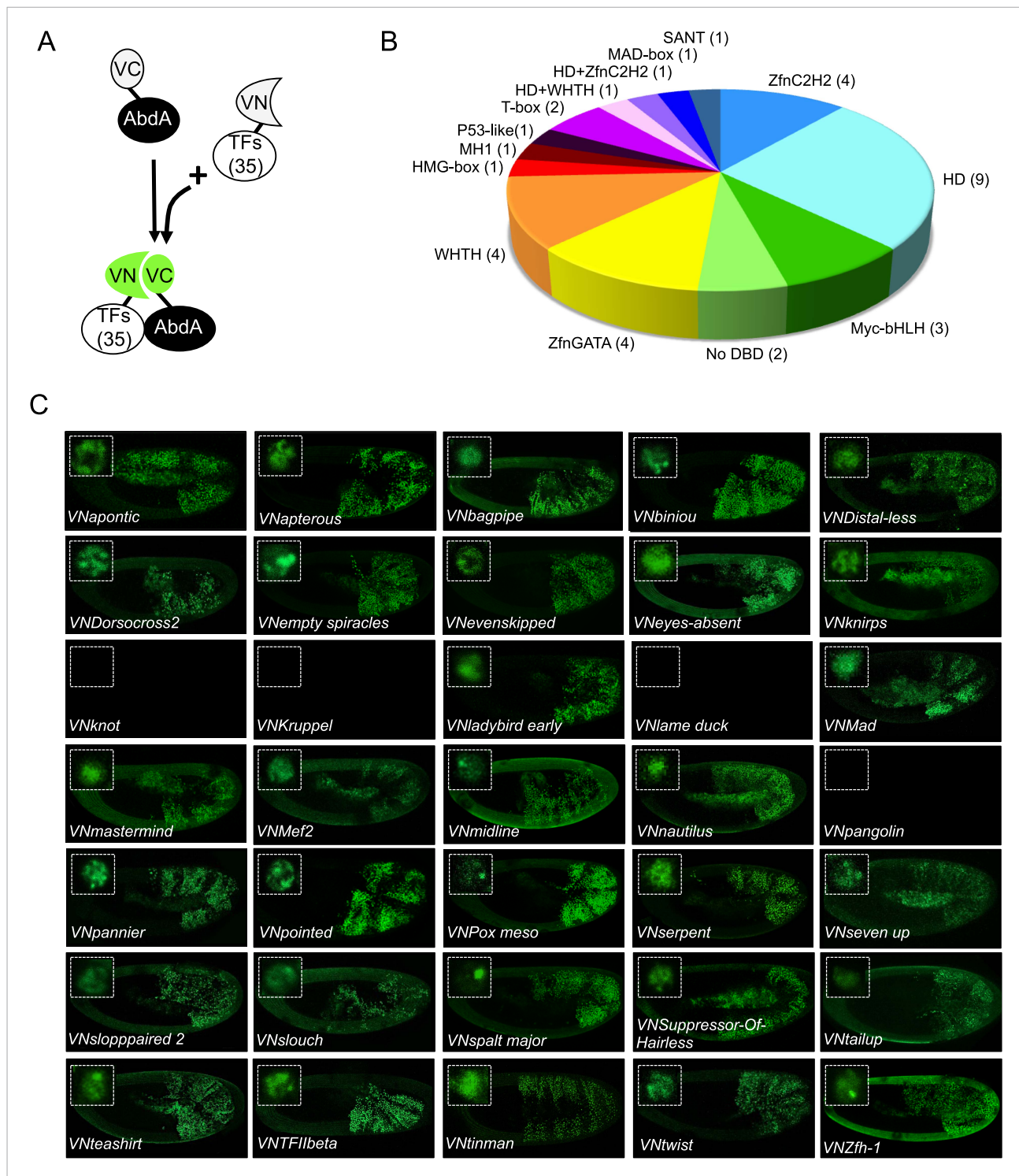
Figure 2. BiFC validates the AbdA-interaction status of competitive TFs. (**A**) Principle of the BiFC screen between AbdA and the 35 selected TFs. (**B**) Repartition of the 35 selected TFs with regard to their DNA-binding domain. (**C**) Illustrative pictures of BiFC signals obtained between VC-AbdA and the indicated VN-TF in the epidermis of stage 10–12 of live embryos. Fusion constructs are expressed with the *abdA-Gal4* driver. Note that typical nuclear interaction profiles are observed between AbdA and different TFs (white-dotted boxes). See also 'Materials and methods', *Supplementary files 2, 3* and *Figure 2—figure supplements 1, 2*.
DOI: 10.7554/eLife.06034.006
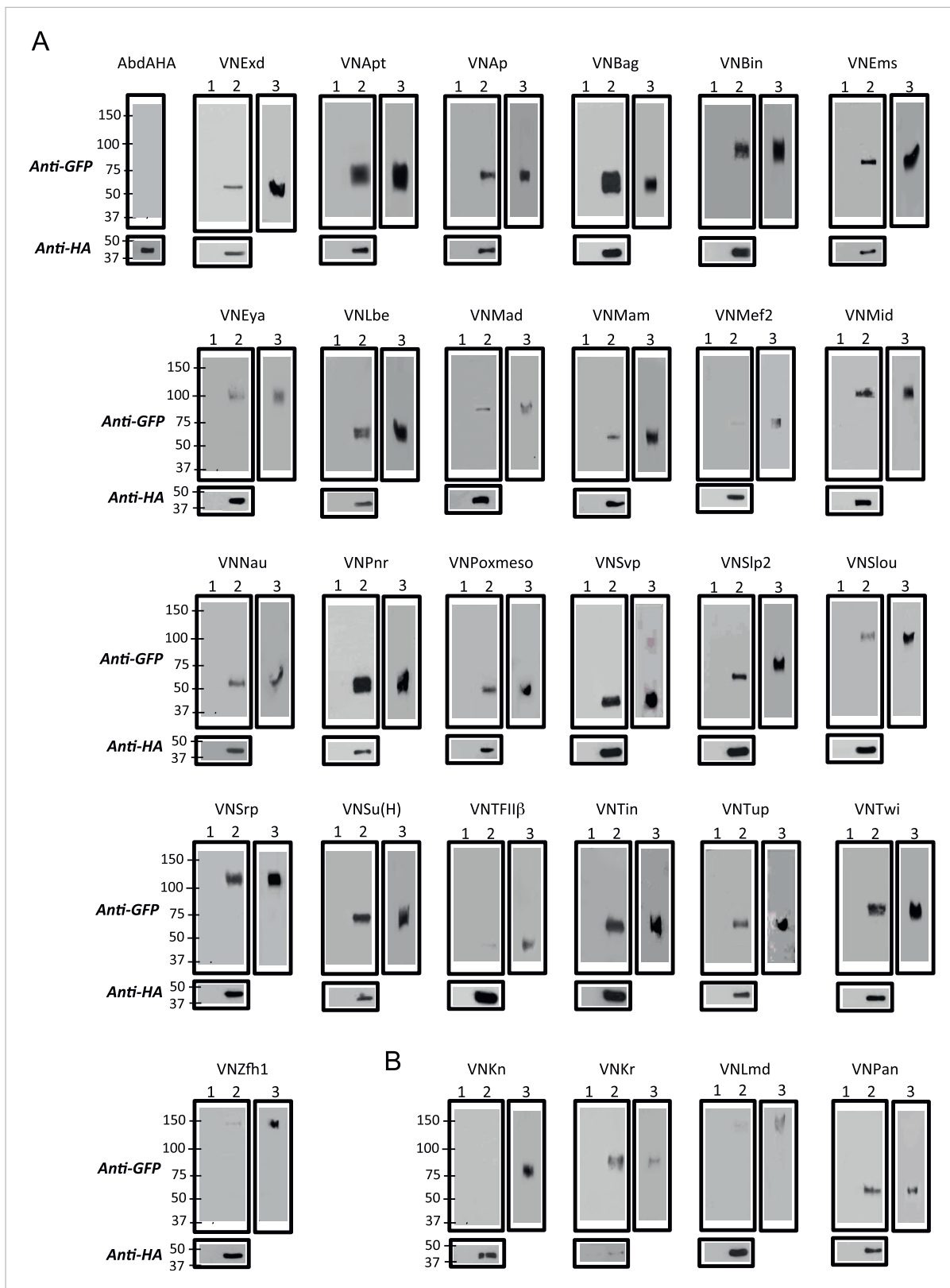
Figure 2—figure supplement 1. Co-immunoprecipitation (co-ip) between AbdA and TFs selected from the set used for BiFC in the *Drosophila* embryo.
(**A**) Positive co-ip experiments. (**B**) Negative co-ip experiments. Co-ips were performed with an anti-HA antibody recognising the AbdA-HA variant.
Figure 2—figure supplement 1. continued on next page

Figure 2—figure supplement 1. Continued

Presence of the TF was revealed with a polyclonal anti-GFP antibody recognising the VN fragment fused to each TF. The ip was performed with the fusion TF expressed alone (lane 1) or together with AbdA (lane 2). Lane 3 corresponds to the input of cells expressing both proteins (20% of the total lysate) before the ip. Gels on the bottom are western blots validating the efficiency of the ip with the anti-HA antibody. First gel corresponds to a control validating that the anti-GFP does not recognize AbdA-HA.
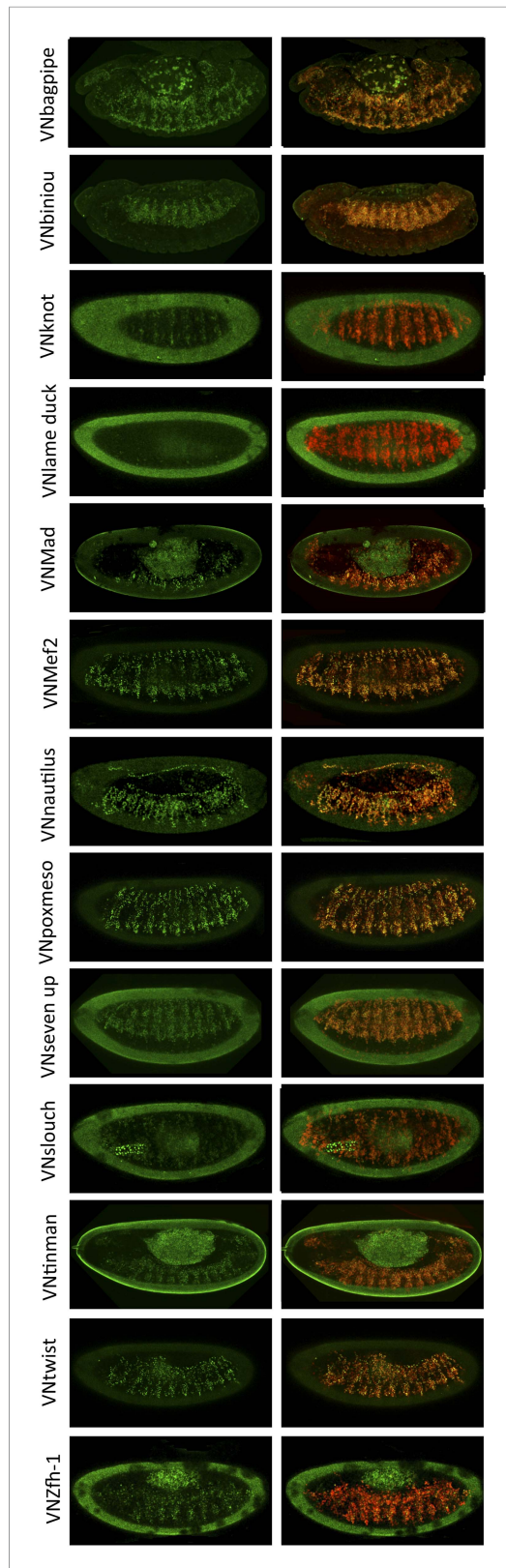
Figure 2—figure supplement 2. BiFC between mesodermal TFs and AbdA in the mesoderm. Fusion
Figure 2—figure supplement 2. continued on next page

Figure 2—figure supplement 2. Continued

proteins were expressed with the *24B-Gal4* driver recombined to *UAS-mCherry* (red), which allows following the expression profile in the mesoderm. BiFC (green) was observed in stages 12–14 of live embryos. Note that weak BiFC signals could be observed with VN-Kn while VN-Lmd remained negative with VC-AbdA.
DOI: 10.7554/eLife.06034.008
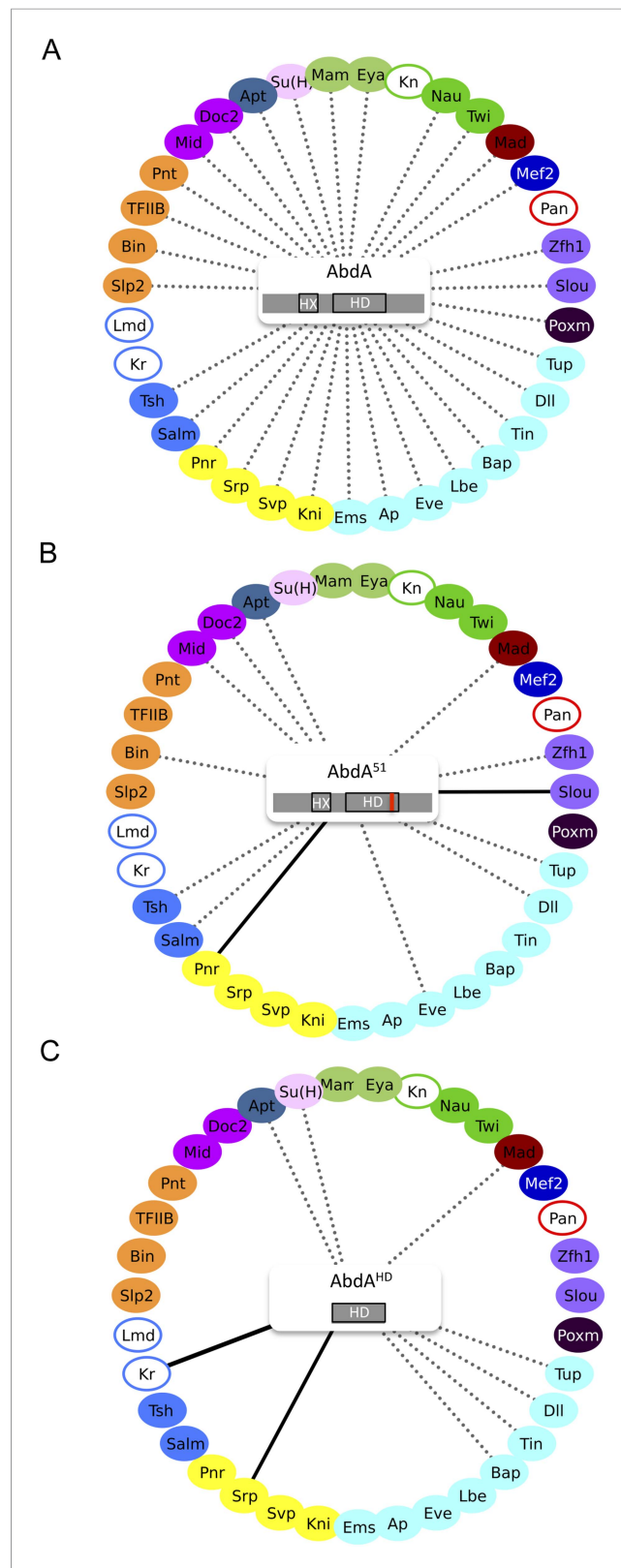
Figure 3. Role of the homeodomain (HD) in the AbdA interactome. (**A**) Interactome with wild type AbdA. (**B**) Interactome with the DNA-binding deficient form of AbdA (mutated in the residue 51 of the HD, as illustrated with the red bar). See also *Figure 3—figure supplement 1*. (**C**) Interactome with the HD of AbdA. *Figure 3. continued on next page*

Figure 3. Continued

See also *Figure 3—figure supplement 2*. Each interactome is represented with the 35 TFs. The colour code for TFs corresponds to their type of DNA-binding domain, as shown in the *Figure 2B*. TFs that are not colour-filled correspond to TFs that do not interact with the wild type Hox protein. Those TFs are not connected to the Hox protein. Dotted lines indicate TFs that do interact with the wild type Hox protein. Interactions with Hox variants are depicted as the following: dotted lines indicate unaffected interactions (in between 51% and 119% of the wild type interaction); solid black lines indicate stronger (equal or superior to 120% of the wild type interaction) or novel interactions (with a non-colour-filled TF); absence of the dotted line with a colour-filled TF indicates a partial (equal or below to 50% of the wild type interaction) or complete loss of the interaction. Each Hox variant is schematized in the centre of the interactome. HD: Homeodomain. HX: Hexapeptide. See also 'Materials and methods'.
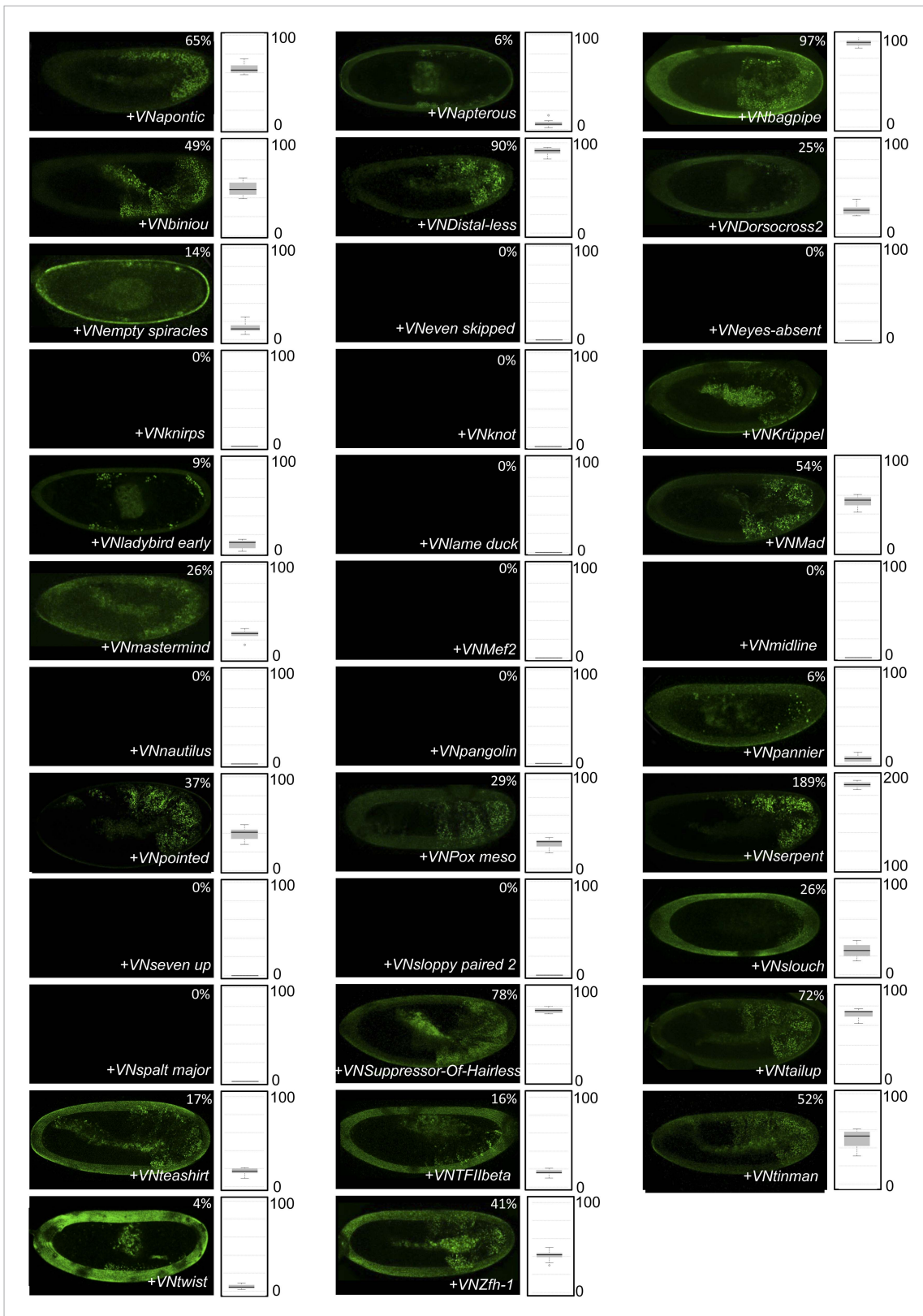DOI: 10.7554/eLife.06034.009
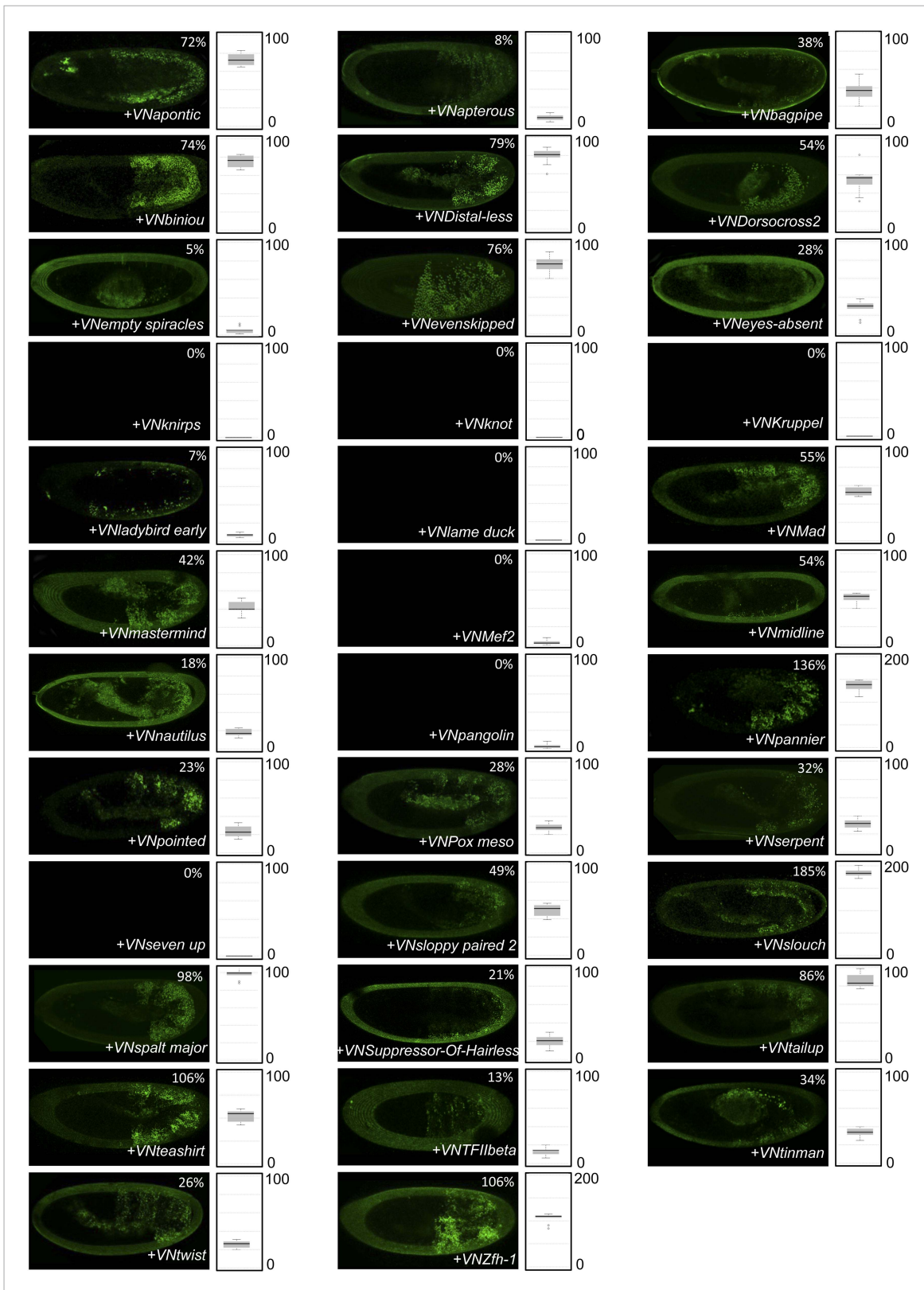
Figure 3—figure supplement 1. BiFC between the 35 TFs and the homeodomain (HD)-mutated form of AbdA. Illustrative pictures are provided for each TF as indicated. Quantifications were performed in the epidermis of stage 10 embryos and are depicted on the right of each picture as a boxplot
Figure 3—figure supplement 1. continued on next page

Figure 3—figure supplement 1. Continued

representation (see also 'Materials and methods'). Illustrative pictures of slightly older embryos are shown when signals were strongly affected. No picture was taken in absence of BiFC.

Figure 3—figure supplement 2. BiFC between the 35 TFs and the homeodomain (HD) of AbdA. Illustrative pictures are provided for each TF as indicated. Quantifications were performed as in *Supplementary file 5*. Illustrative pictures of slightly older embryos are shown when signals

Figure 3—figure supplement 2. continued on next page

Figure 3—figure supplement 2. Continued

were strongly affected. No statistical quantification is provided in the case of a new interaction (as seen with Krüppel). No picture was taken in absence of BiFC.
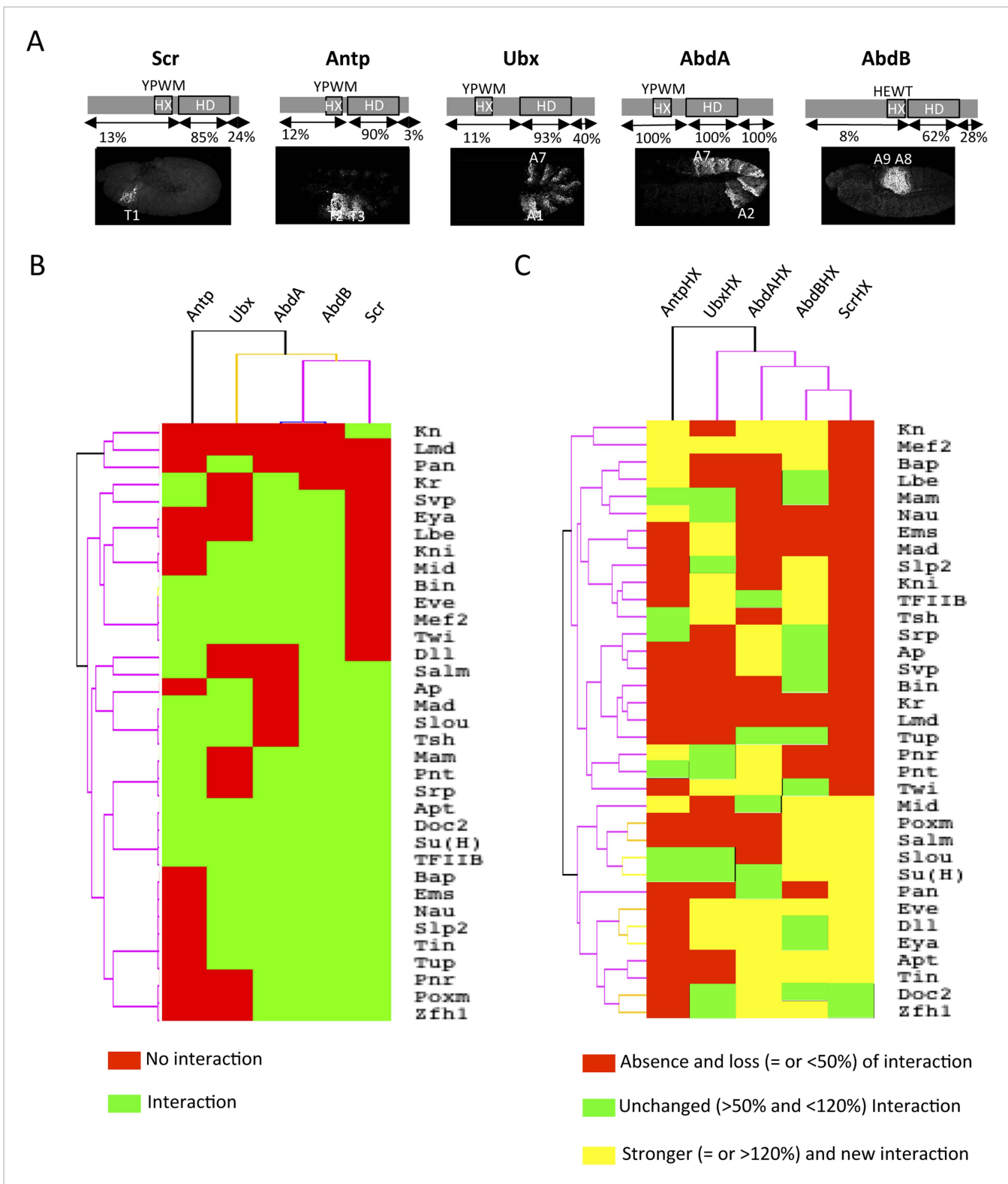
Figure 4. Comparison between wild type and Hexapeptide(HX)-mutated Hox interactomes. (**A**) Embryonic expression profile (grey) and protein sequence identity of each of the five *Drosophila* Hox proteins under study. The percentage of sequence identity is given in comparison to AbdA. The conserved core sequence of the HX is also given for each Hox protein. (**B**) Heatmap showing the organisation of wild type Hox interactomes with the 35 TFs. See also *Figure 4—figure supplements 1–4*. (**C**) Heatmap showing the organisation of HX-mutated Hox interactomes with the 35 TFs. See also *Figure 4—figure supplements 5–9*. Interactions are symbolized by a colour code, as indicated. Note that the yellow colour, which corresponds to a gain of the interaction
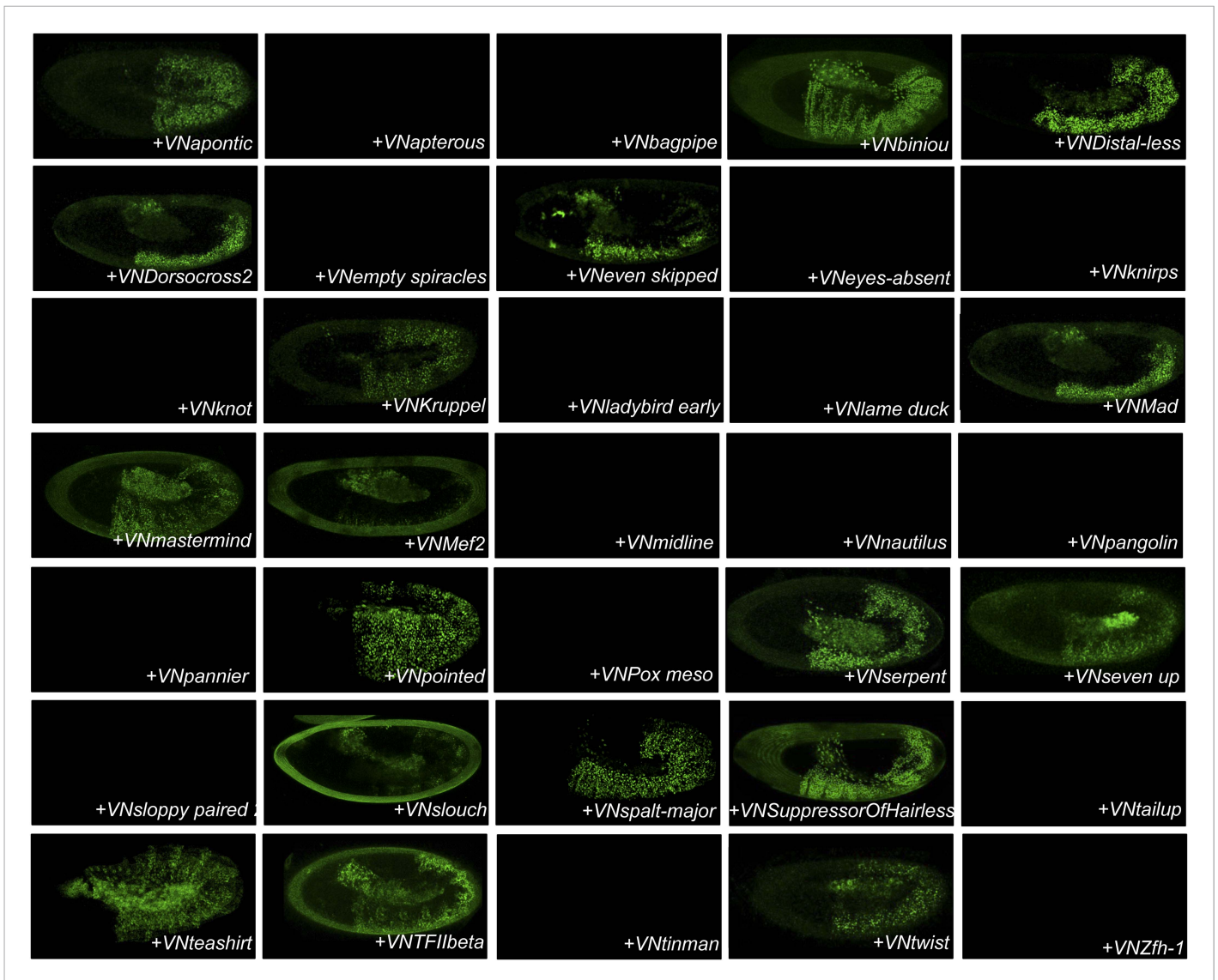
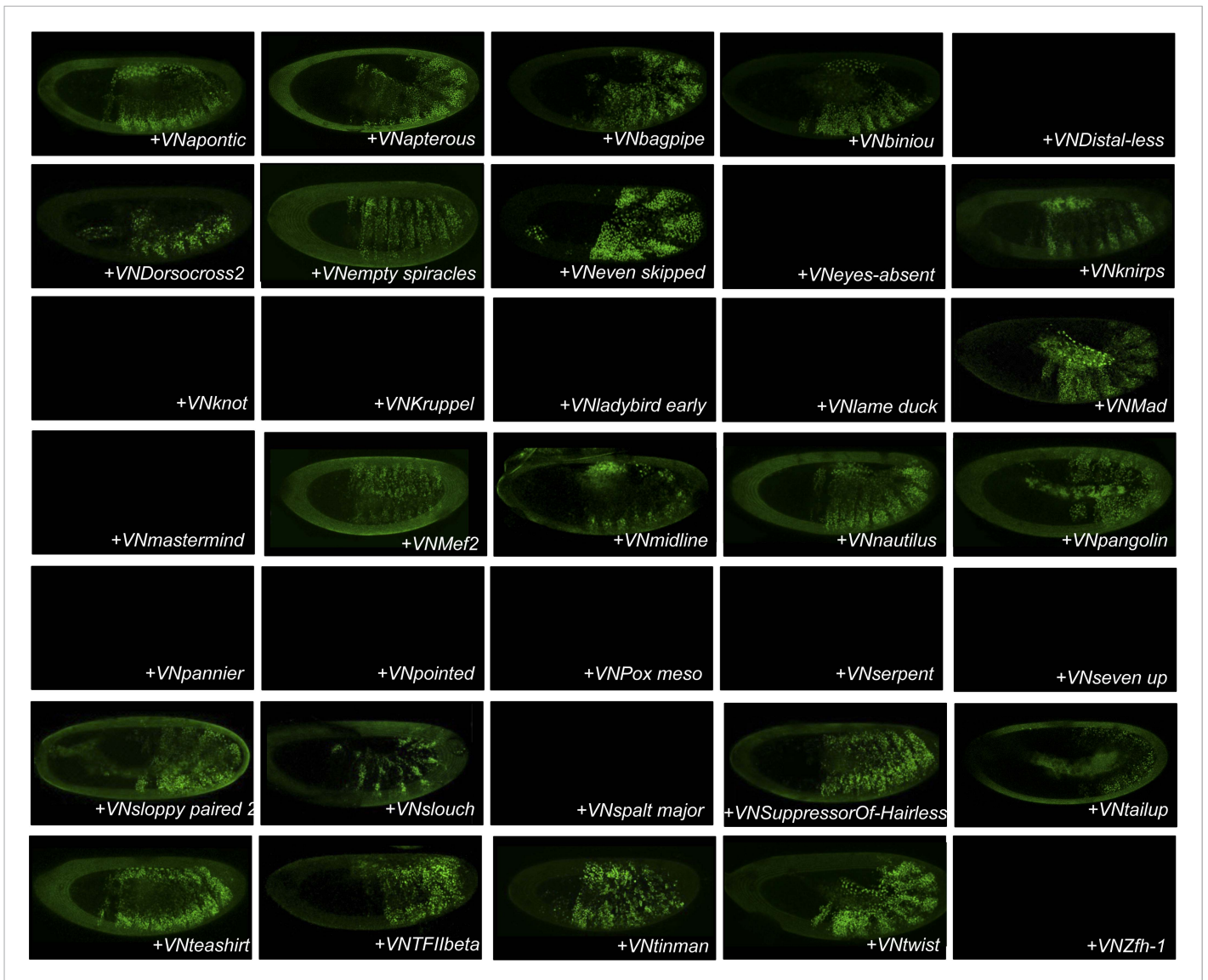*Figure 4. continued on next page*
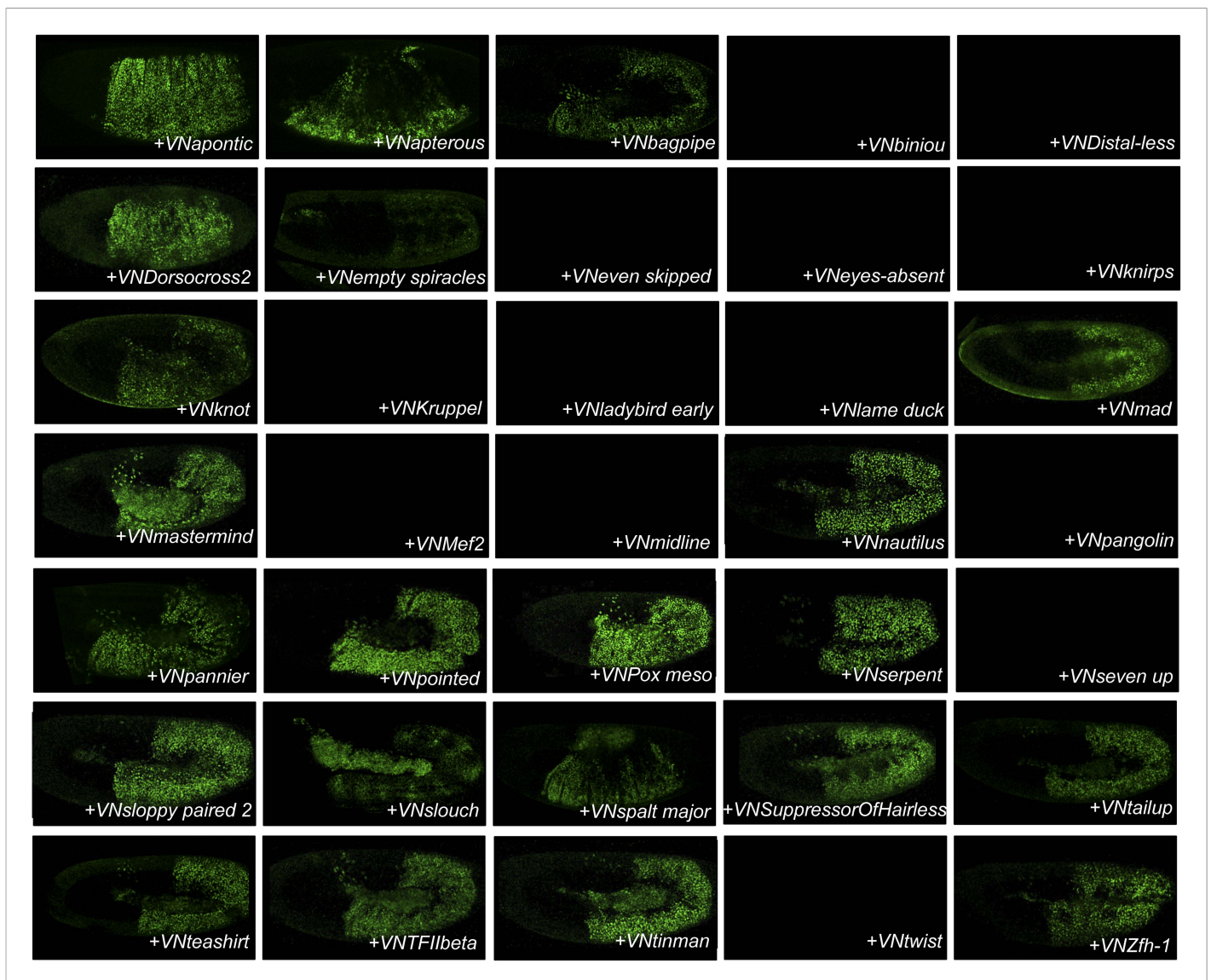
Figure 4—figure supplement 1. BiFC between the 35 TFs and Sex combs reduced (Scr). Illustrative pictures of stage 10–12 embryos are provided for each TF as indicated.
DOI: 10.7554/eLife.06034.013

Figure 4—figure supplement 2. BiFC between the 35 TFs and Antennapedia (Antp). Illustrative pictures of stage 10–12 embryos are provided for each TF as indicated.
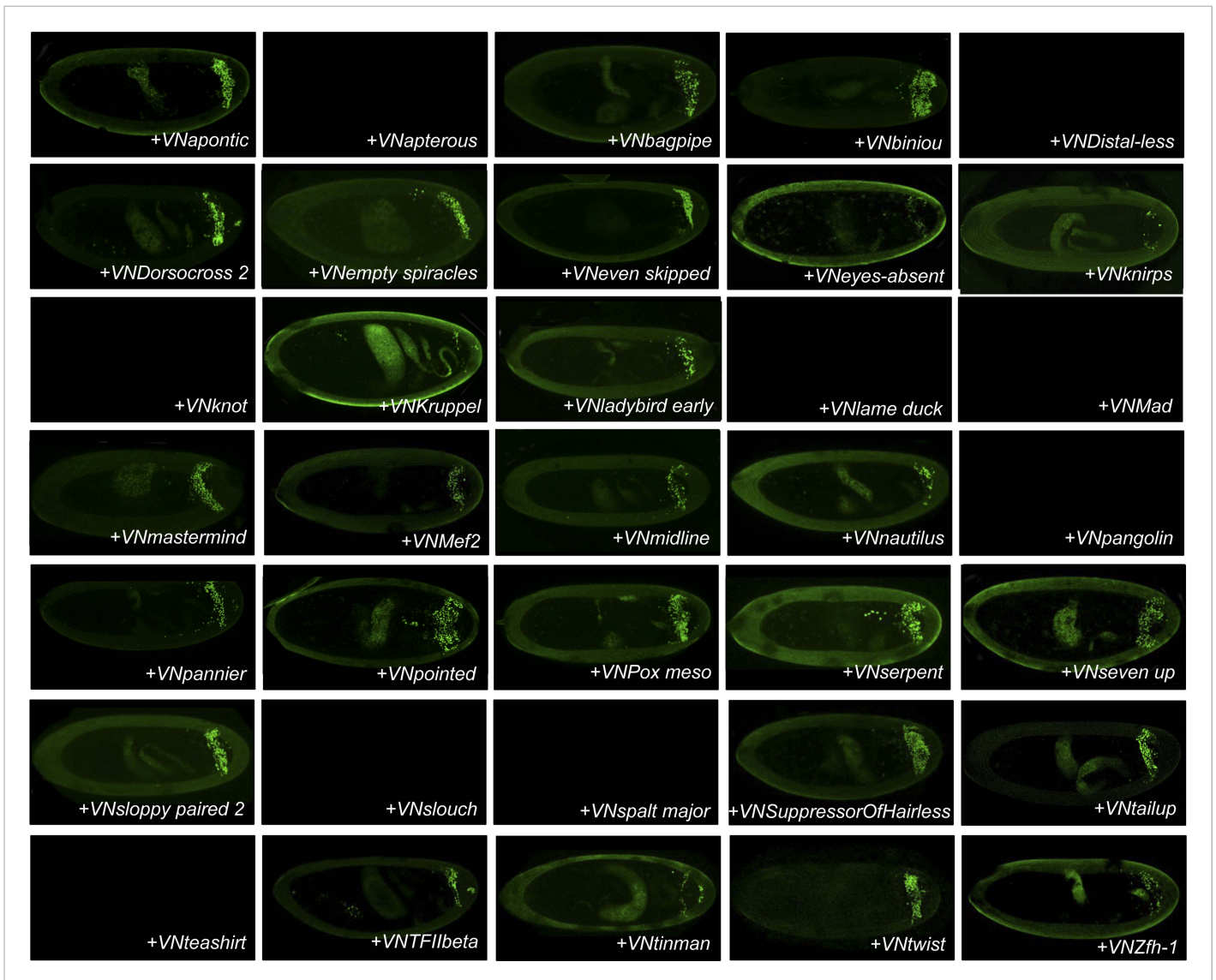
DOI: 10.7554/eLife.06034.014

Figure 4—figure supplement 3. BiFC between the 35 TFs and Ultrabithorax (Ubx). Illustrative pictures of stage 10–12 embryos are provided for each TF as indicated.
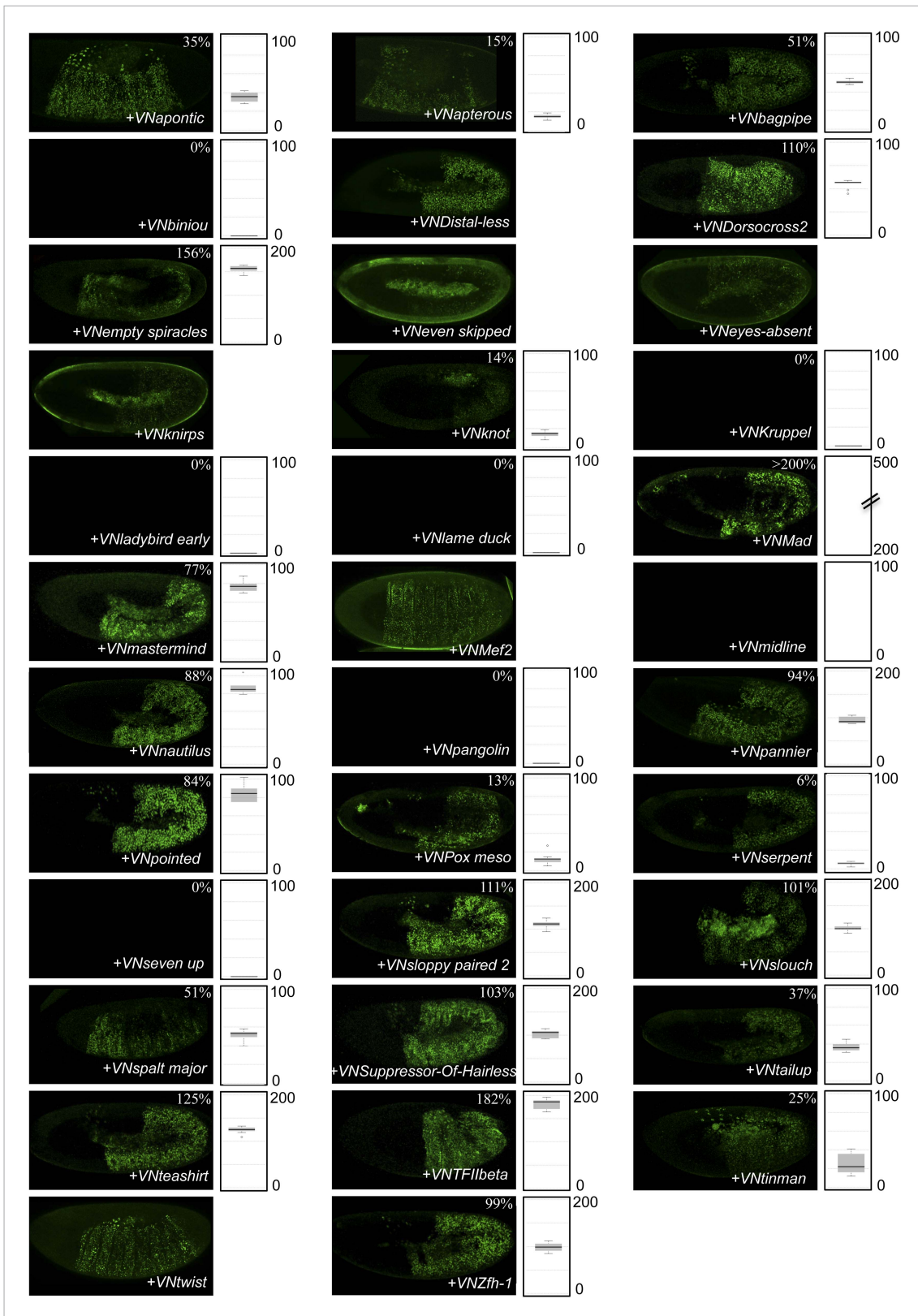DOI: 10.7554/eLife.06034.015

Figure 4—figure supplement 4. BiFC between the 35 TFs and AbdominalB (AbdB). Illustrative pictures of stage 10–12 embryos are provided for each TF as indicated.
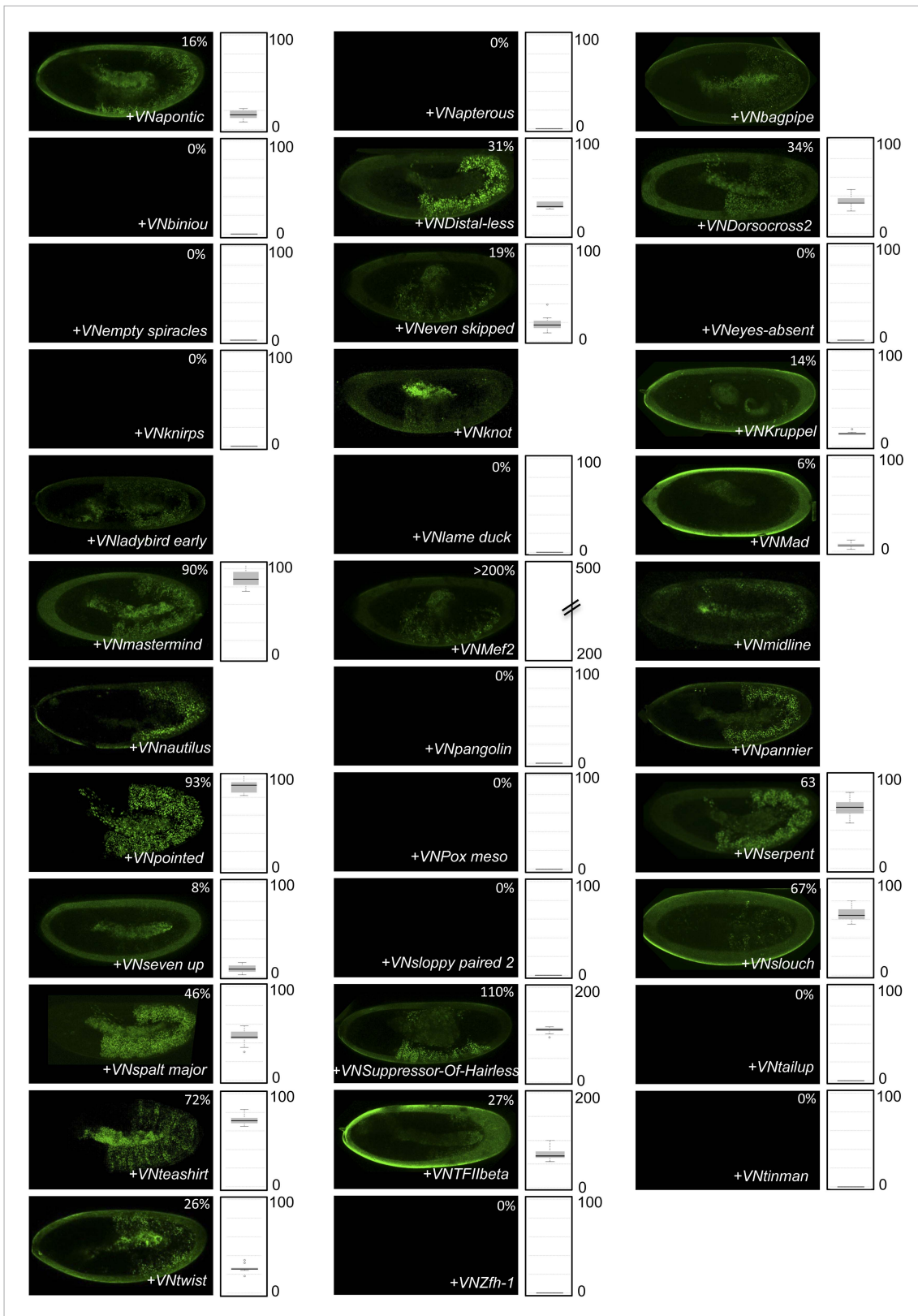
DOI: 10.7554/eLife.06034.016

Figure 4—figure supplement 5. BiFC between the 35 TFs and hexapeptide (HX)-mutated Scr. Illustrative pictures of stage 10–12 embryos are provided for each TF as indicated. Quantification was performed as in **Figure 3—figure supplement 1**. Illustrative pictures of slightly older embryos are shown *Figure 4—figure supplement 5. continued on next page*

Figure 4—figure supplement 5. Continued

when signals were strongly affected. No picture was taken in absence of BiFC. No statistical quantification is provided in the case of a new interaction (as seen for Distal-less, Even skipped, Eyes-absent, Knirps, Mef2 and Twist).
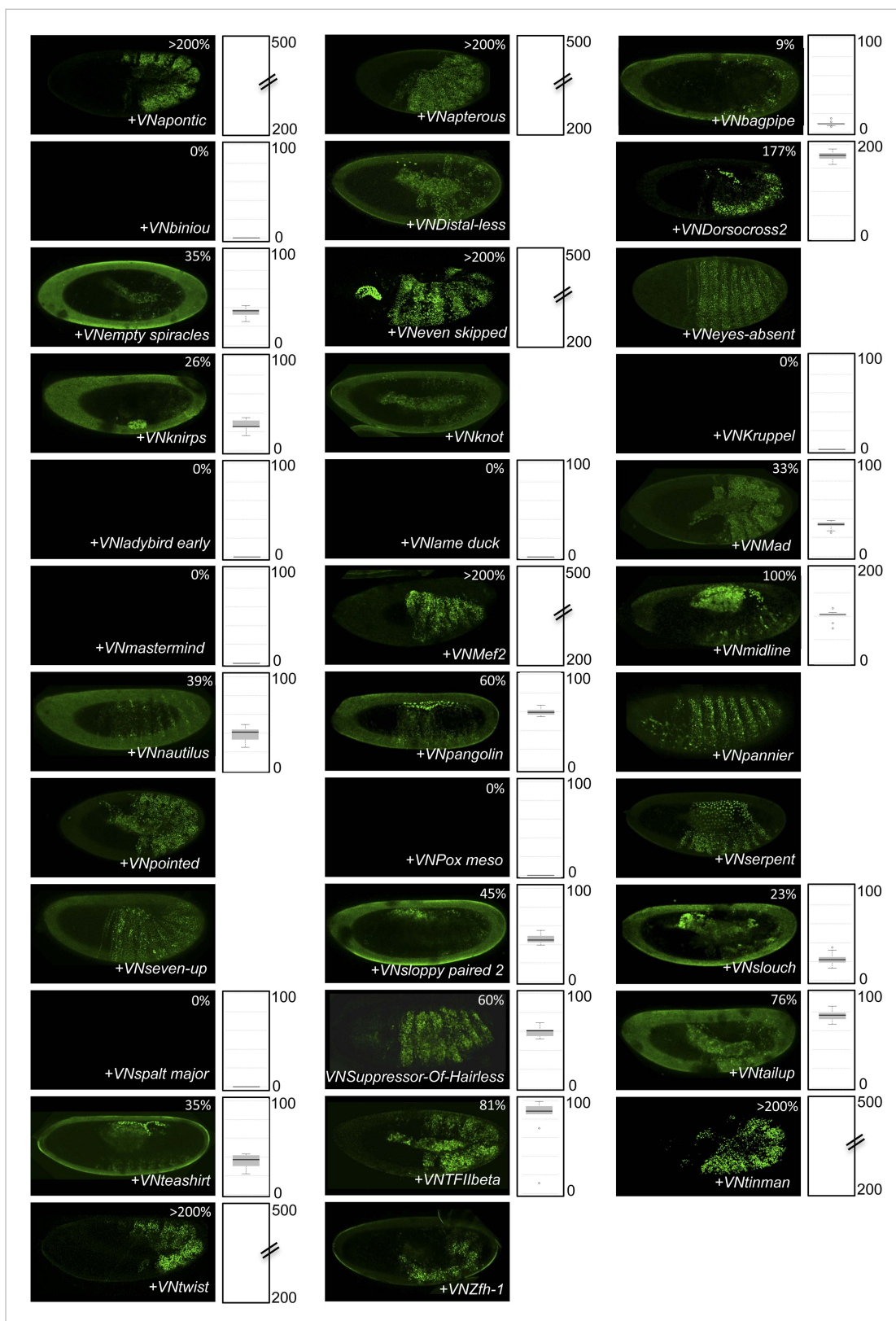
Figure 4—figure supplement 6. BiFC between the 35 TFs and hexapeptide (HX)-mutated Antp. Illustrative pictures of stage 10–12 embryos are provided for each TF as indicated. Quantification was performed as in *Figure 3—figure supplement 1*. Illustrative pictures of slightly older embryos are shown *Figure 4—figure supplement 6. continued on next page*

Figure 4—figure supplement 6. Continued

when signals were strongly affected. No picture was taken in absence of BiFC. No statistical quantification is provided in the case of a new interaction (as seen for Bagpipe, Knot, Ladybird early, Midline, Nautilus and Pannier).
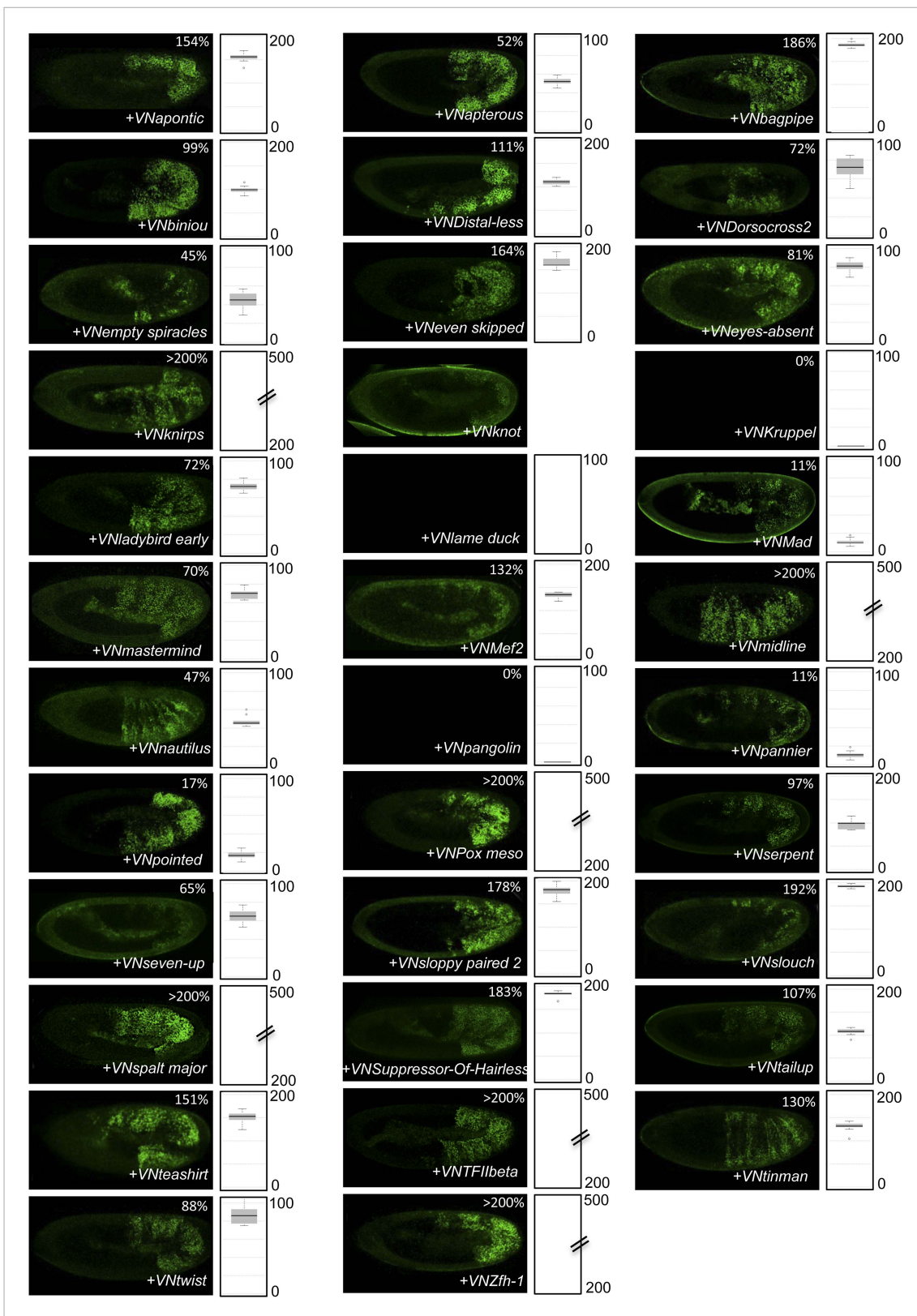
Figure 4—figure supplement 7. BiFC between the 35 TFs and hexapeptide (HX)-mutated Ubx. Illustrative pictures of stage 10–12 embryos are provided for each TF as indicated. Quantification was performed as in *Figure 3—figure supplement 1*. Illustrative pictures of slightly older embryos are shown *Figure 4—figure supplement 7. continued on next page*

Figure 4—figure supplement 7. Continued

when signals were strongly affected. No picture was taken in absence of BiFC. No statistical quantification is provided in the case of a new interaction (as seen for Distal-less, Eyes-absent, Knot, Pannier, Pointed, Serpent, Seven-up and Zfh-1).
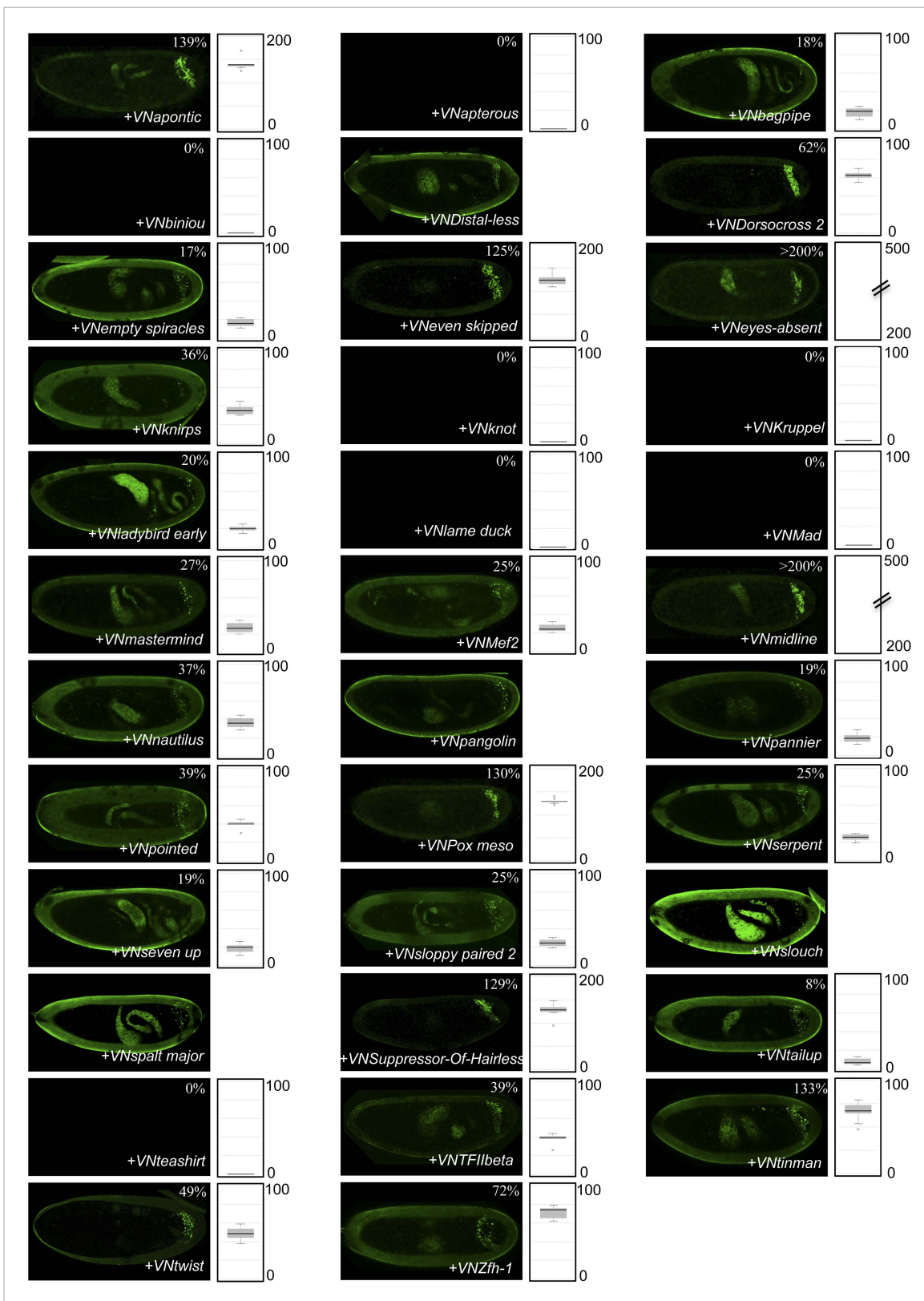
Figure 4—figure supplement 8. BiFC between the 35 TFs and hexapeptide (HX)-mutated AbdA. Illustrative pictures of stage 10–12 embryos are provided for each TF as indicated. Quantification was performed as in **Figure 3—figure supplement 1**. Illustrative pictures of slightly older embryos are *Figure 4—figure supplement 8*. continued on next page

Figure 4—figure supplement 8. Continued

shown when signals were strongly affected. No picture was taken in absence of BiFC. No statistical quantification is provided in the case of a new interaction (as seen for Knot).

Figure 4—figure supplement 9. BiFC between the 35 TFs and hexapeptide (HX)-mutated AbdB. Illustrative pictures of stage 10–12 embryos are provided for each TF as indicated. Quantification was performed as in *Figure 3—figure supplement 1*. Illustrative pictures of slightly older embryos are *Figure 4—figure supplement 9. continued on next page*

Figure 4—figure supplement 9. Continued

shown when signals were strongly affected. No picture was taken in absence of BiFC. No statistical quantification is provided in the case of a new interaction (as seen for Distal-less, Pangolin, Slouch and Spalt major).
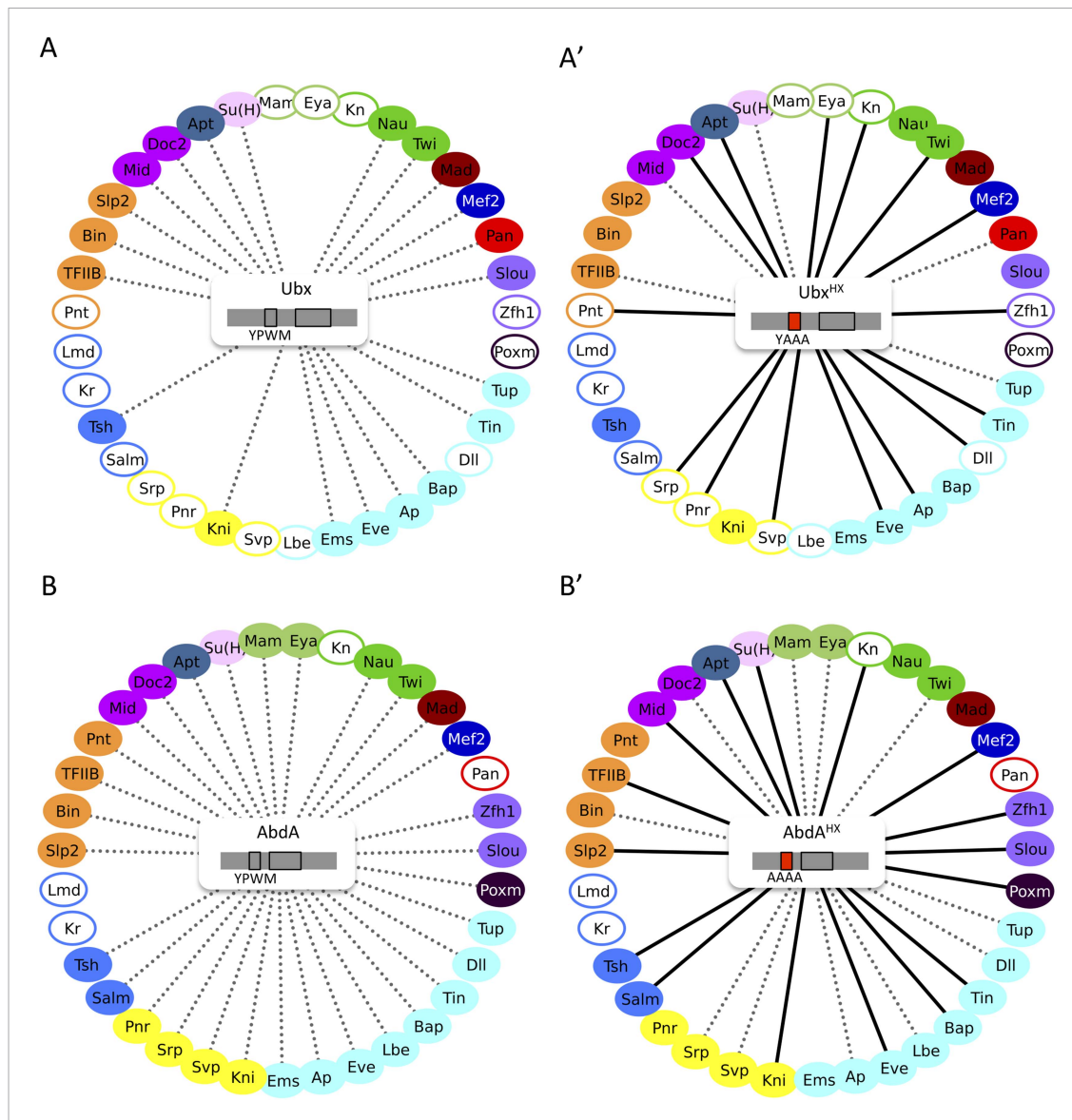
Figure 5. The HX mutation increases the interaction potential of Hox proteins with TFs in vivo: example in Ubx and AbdA. (**A–A′**) Comparison between wild type and HX-mutated interactomes of Ubx. (**B–B′**) Comparison between wild type and HX-mutated interactomes of AbdA. The HX mutation led more frequently to stronger or new interactions than to interaction loses in these two Hox proteins. Colour code and representation are as in *Figure 3*. The HX mutation is indicated and highlighted in red. See also *Figure 5—figure supplement 1*.
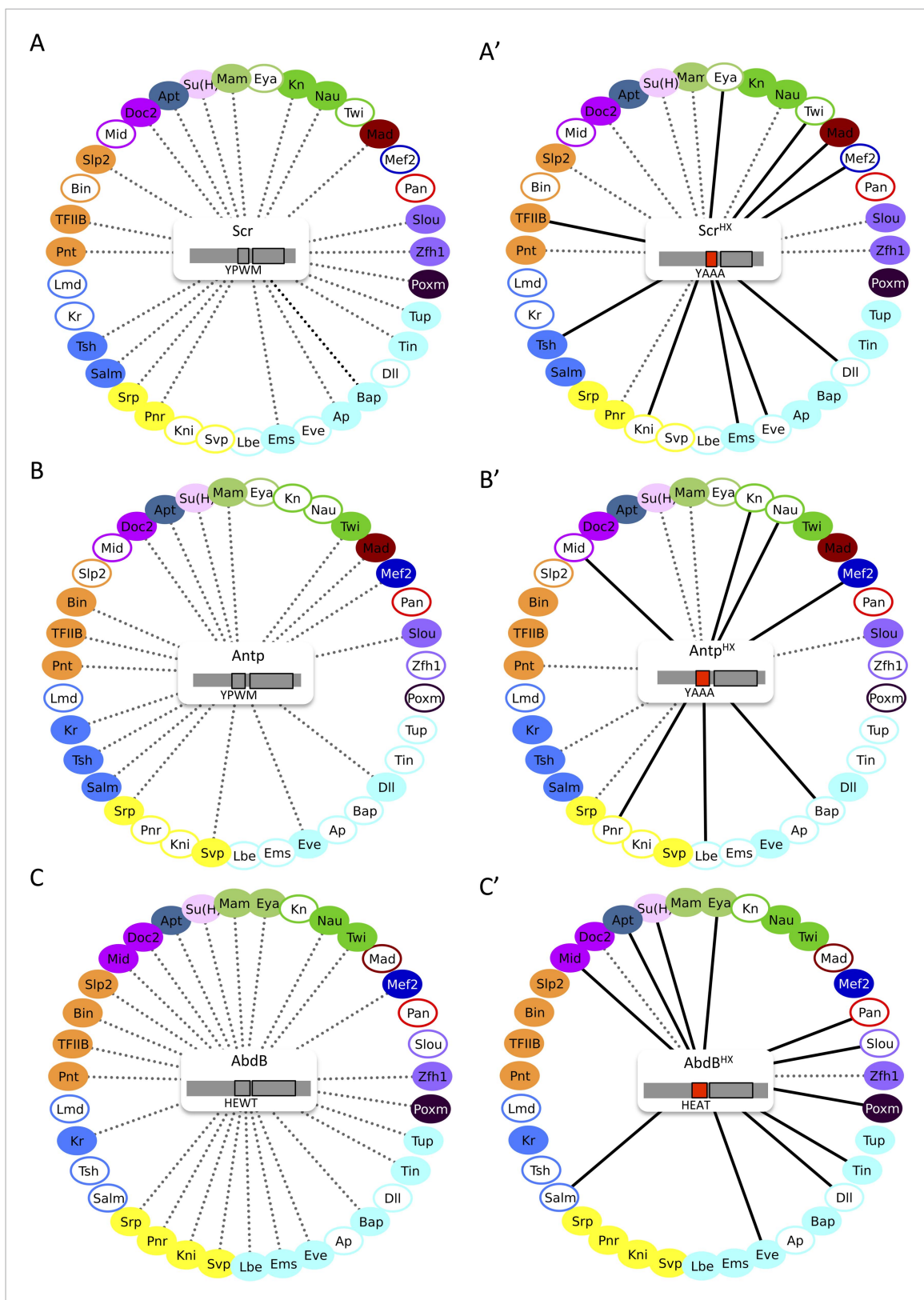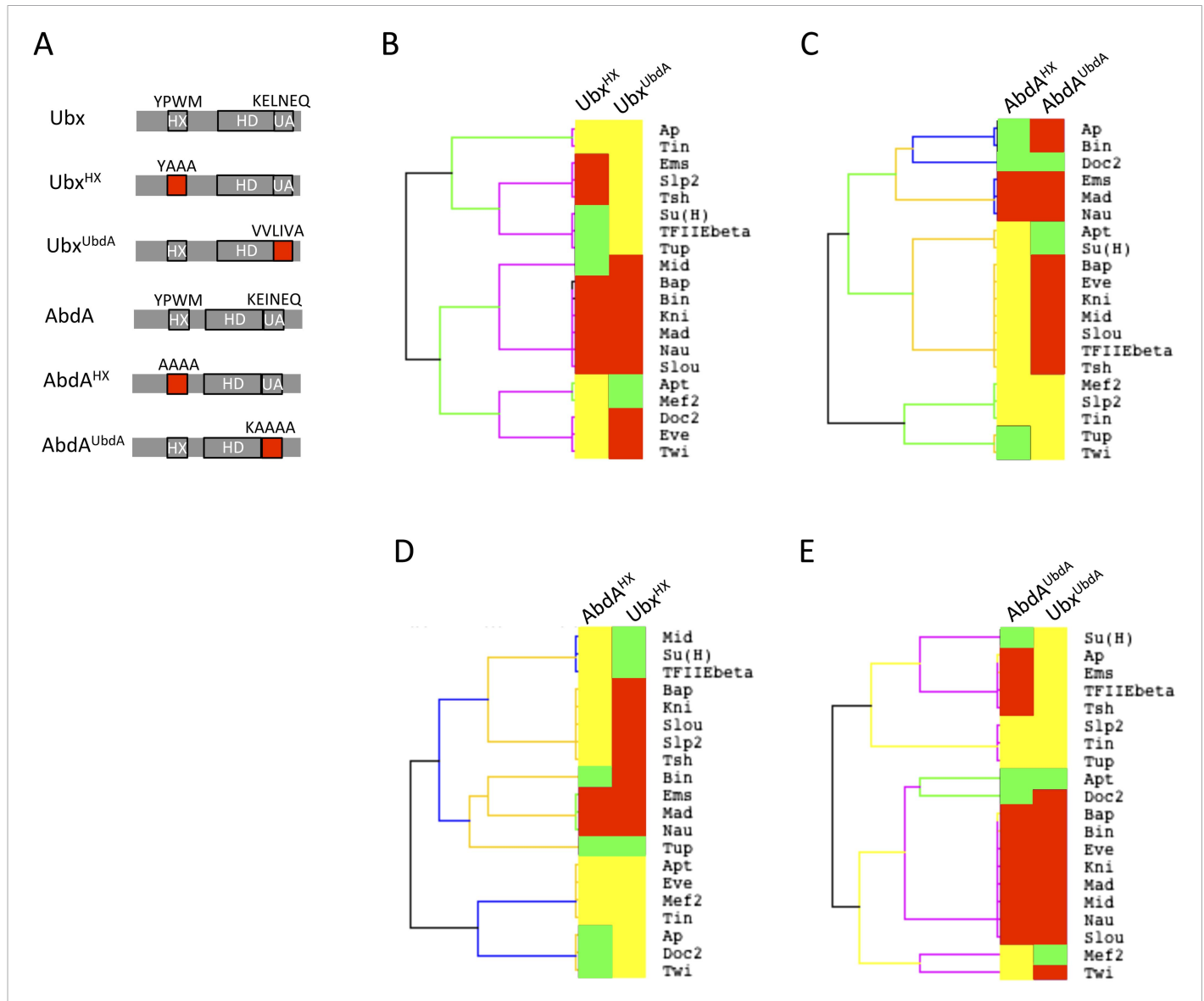
Figure 5—figure supplement 1. The HX mutation increases the interaction potential of Hox proteins with TFs in vivo: example in Scr, Antp, and AbdB. (**A**–**A'**) Comparison between wild type and HX-mutated Scr. (**B**–**B'**) Comparison between wild type and HX-mutated Antp. (**C**–**C'**) Comparison

*Figure 5—figure supplement 1. continued on next page*

Figure 6. Usage mode of the HX and UbdA motifs in Ubx and AbdA proteins. (**A**) Schematic representation of wild type and HX- or UbdA-mutated Ubx and AbdA proteins. (**B**) Heatmap comparing interaction properties of HX- and UbdA-mutated Ubx proteins with a set of 20 TFs. These TFs are common to Ubx and AbdA for BiFC. See also **Figure 6—figure supplement 1**. (**C**) Heatmap comparing interaction properties of HX- and UbdA-mutated AbdA proteins with the same set of TFs. See also **Figure 6—figure supplement 2**. Note that the HX and UbdA mutations have distinct or opposite effects for most of the interactions in Ubx and AbdA. (**D**) Heatmap comparing interaction properties of HX-mutated Ubx and AbdA proteins with the 20 common TFs. (**E**) Heatmap comparing interaction properties of UbdA-mutated Ubx and AbdA proteins with the 20 common TFs. Note that a higher proportion of TFs is similarly affected by the UbdA mutation in Ubx and AbdA when compared to the HX mutation. Colour code is as in **Figure 4**.

DOI: 10.7554/eLife.06034.024
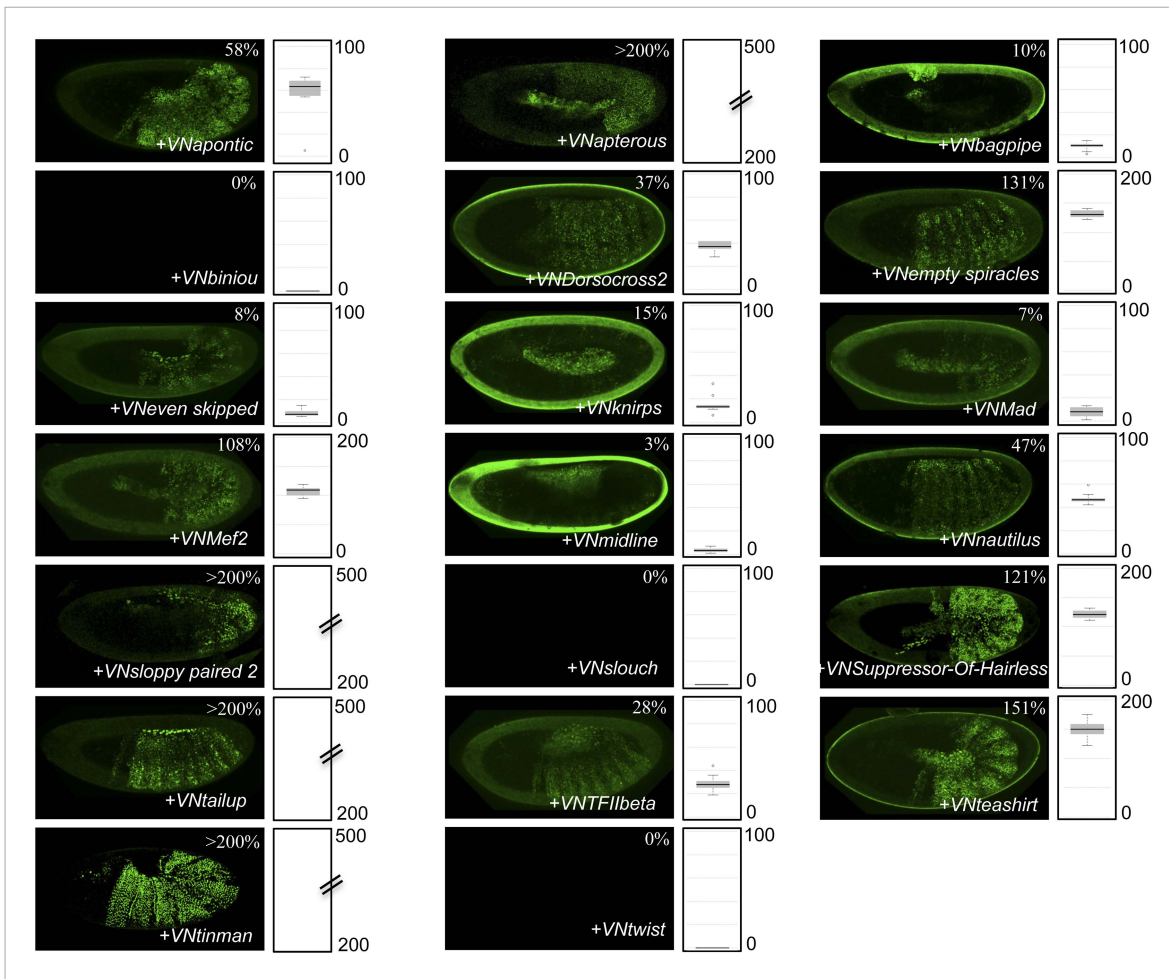
Figure 6—figure supplement 1. BiFC with UbdA-mutated Ubx in the epidermis. BiFC was performed with the 20 TFs interacting both with Ubx and AbdA. Quantification was performed as in **Figure 3—figure supplement 1**. Illustrative pictures of slightly older embryos are shown when signals were strongly affected. No picture was taken in absence of BiFC.
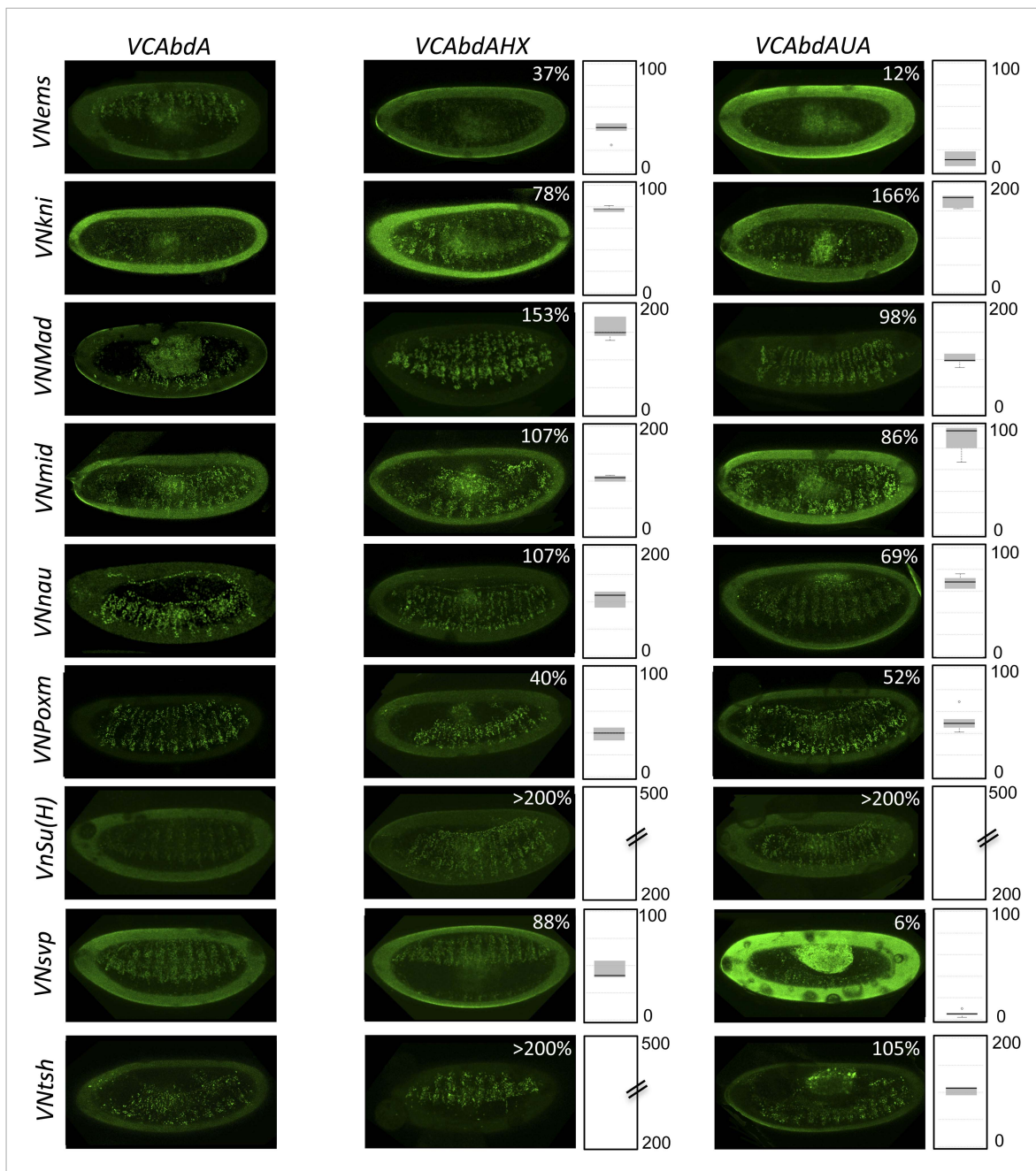
DOI: 10.7554/eLife.06034.025
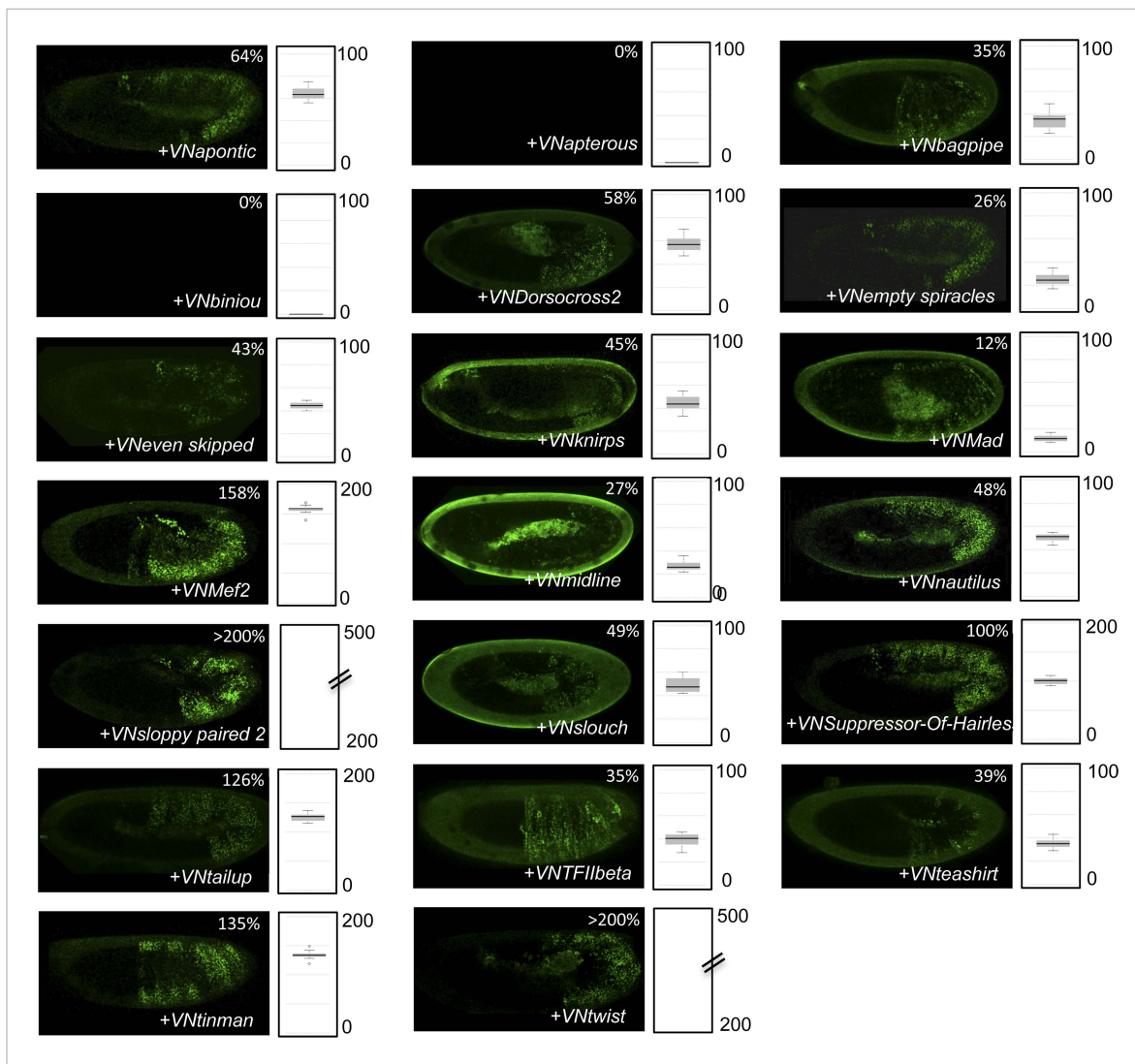
Figure 6—figure supplement 2. BiFC with UbdA-mutated AbdA in the epidermis. BiFC was performed with the 20 TFs interacting both with Ubx and AbdA. Quantification was performed as in *Figure 3—figure supplement 1*. Illustrative pictures of slightly older embryos are shown when signals were strongly affected. No picture was taken in absence of BiFC.
DOI: 10.7554/eLife.06034.026
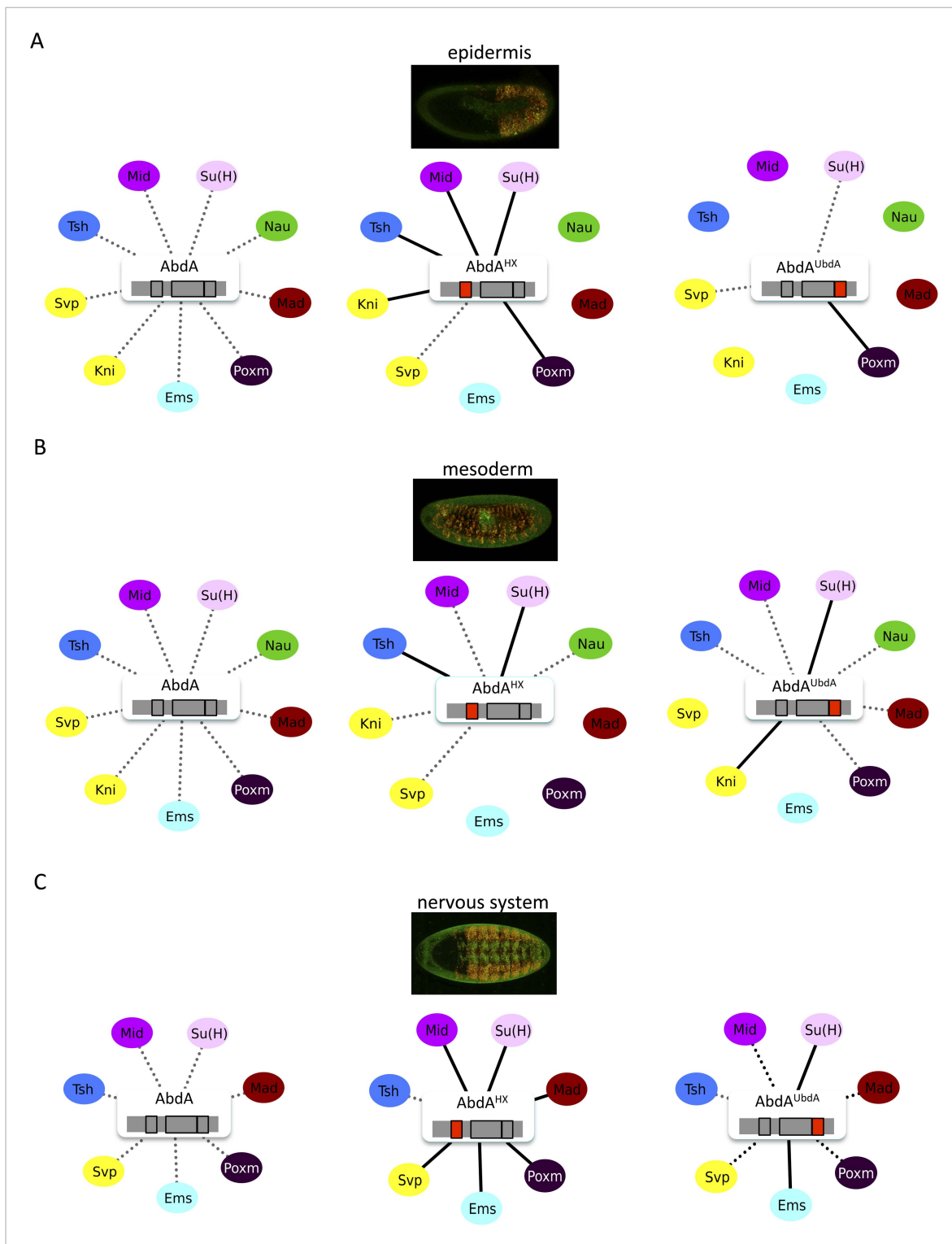
Figure 7. The HX and UbdA motifs of AbdA have different interaction properties in different embryonic tissues. (**A**) Interaction properties of wild type and HX- or UbdA-mutated AbdA in the epidermis. (**B**) Interaction properties of wild type and HX- or UbdA-mutated AbdA in the mesoderm. See also **Figure 7—figure supplement 1**. (**C**) Interaction properties of wild type and HX- or UbdA-mutated AbdA in the nervous system. See also **Figure 7—figure supplement 2**. Picture of an embryo making BiFC (green) and expressing the dsRed fluorescent protein under the control of the Gal4 driver illustrates the tissue of interest in each condition. Interactomes are represented as in **Figure 3**.
DOI: 10.7554/eLife.06034.027

Figure 7—figure supplement 1. BiFC with wild type, HX- or UbdA-mutated AbdA in the mesoderm. BiFC was performed with a set of 9 TFs that were all BiFC-positive with AbdA in the epidermis. Statistical quantification of BiFC signals with mutated AbdA proteins is shown as a boxplot representation. Quantification was performed in the mesoderm of stage 12 embryos (see also 'Materials and methods').
DOI: 10.7554/eLife.06034.028
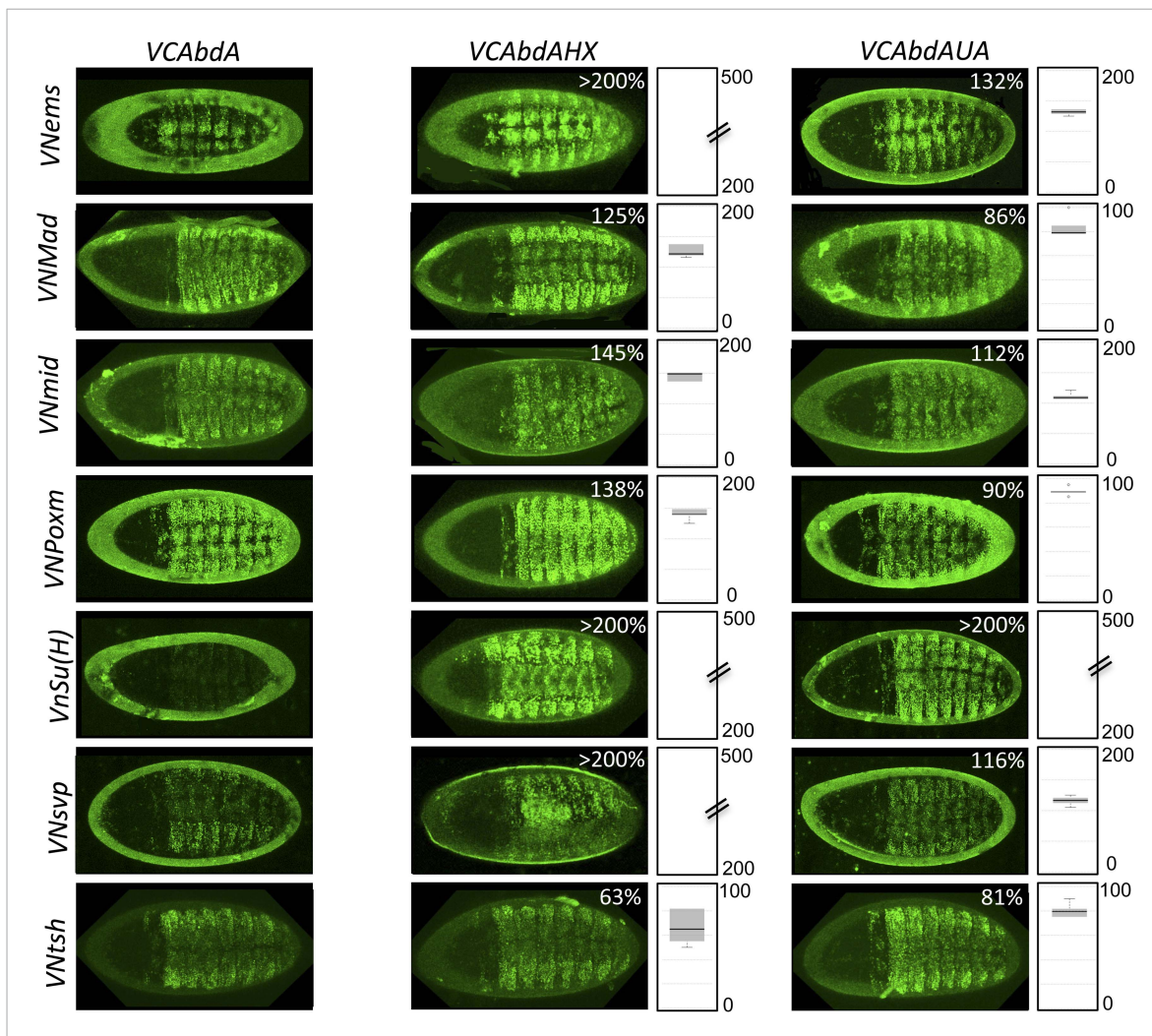
Figure 7—figure supplement 2. BiFC with wild type, HX- or UbdA-mutated AbdA in the nervous system. BiFC was performed with a set of seven TFs that were all BiFC-positive with AbdA in the epidermis. Statistical quantification of BiFC signals with mutated AbdA proteins is shown as a boxplot representation. Quantification was specifically performed in the ventral nerve cord of stage 14 of live embryos (see also 'Materials and methods').
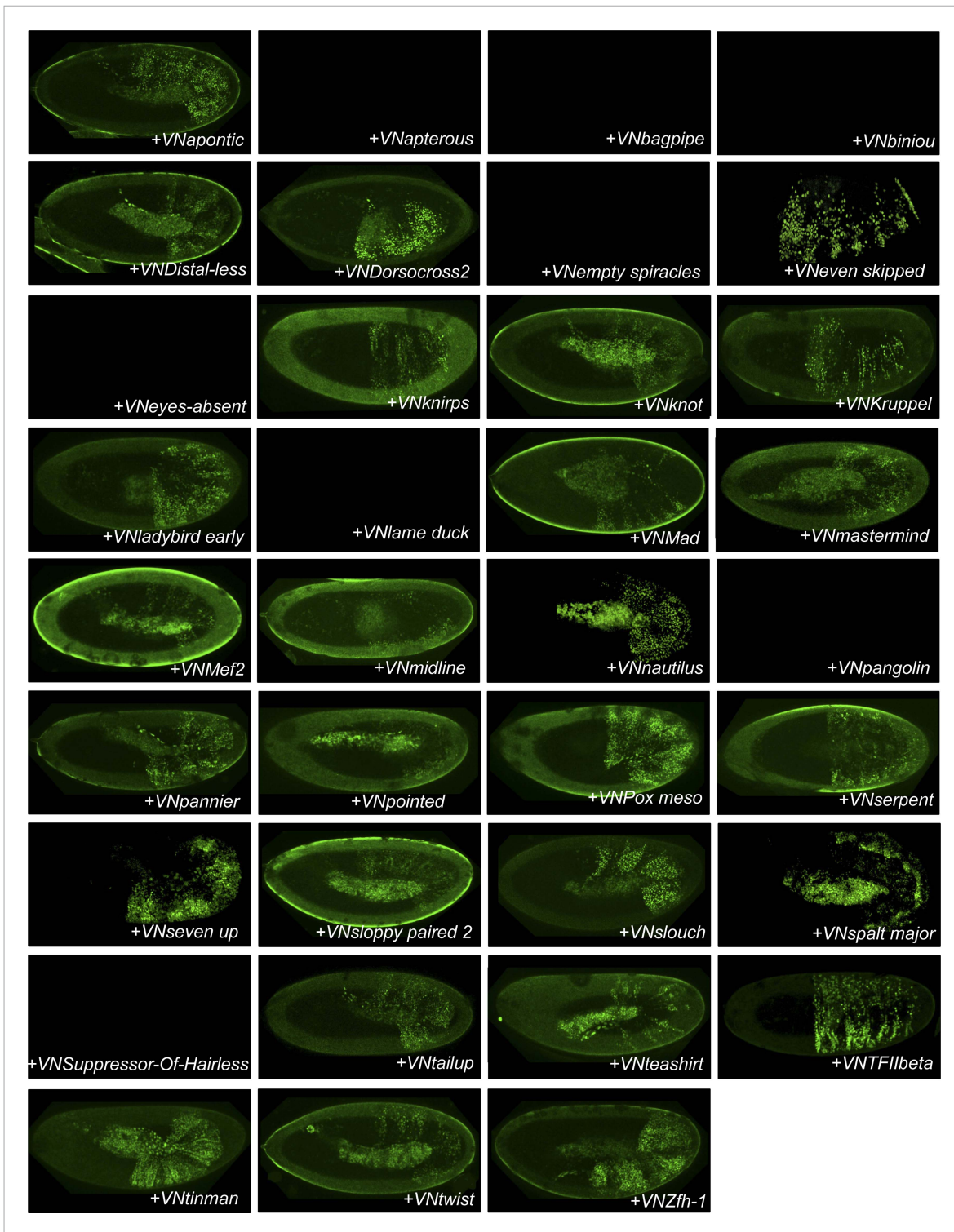DOI: 10.7554/eLife.06034.029
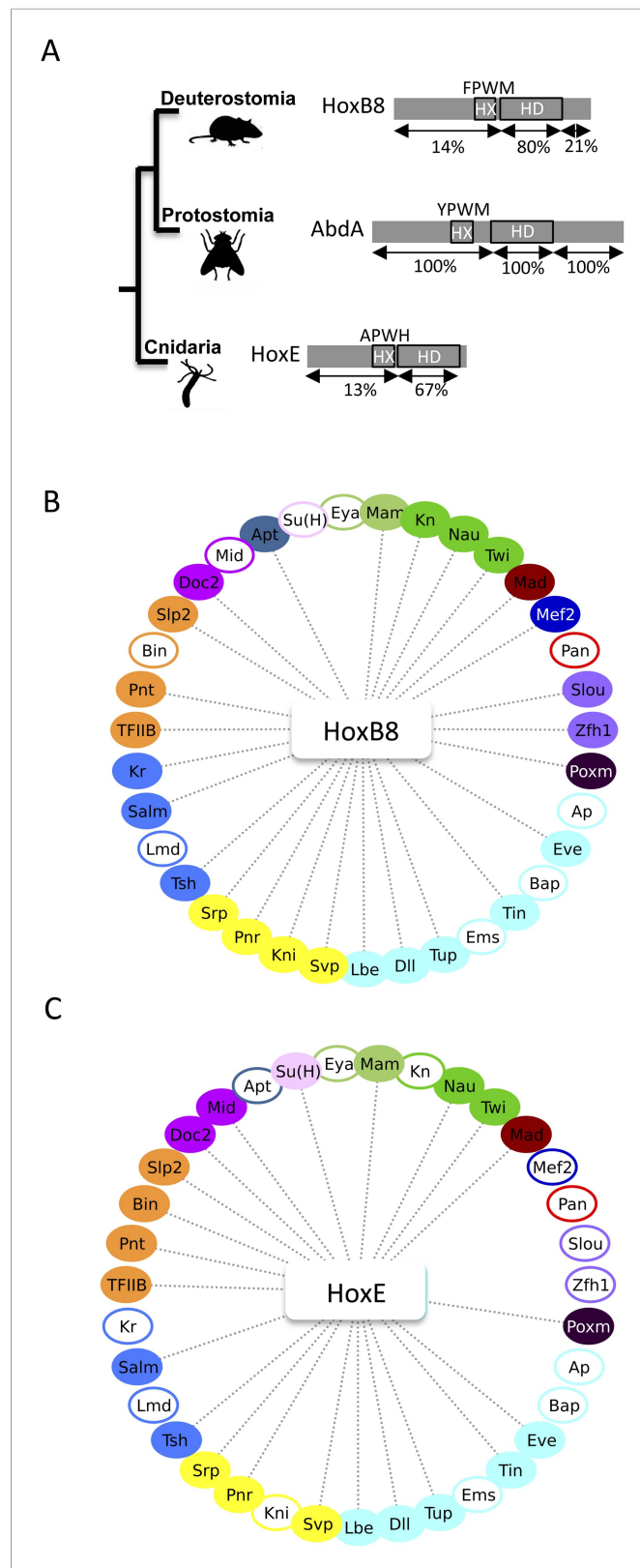
Figure 8. The *Nematostella* HoxE and mouse HoxB8 proteins interact with several *Drosophila* TFs. (**A**) Schematic representations of the Hox proteins and the corresponding animal phylogeny. The percentage of sequence identity is given in comparison to AbdA. (**B**) Interactome between mouse HoxB8 and the 35 *Drosophila* TFs. (**C**) Interactome

Figure 8. continued on next page

Figure 8. Continued

between *Nematostella* HoxE and the 35 *Drosophila* TFs. Colour code and representation are as in **Figure 3**. See also **Figure 8—figure supplements 1–5**.
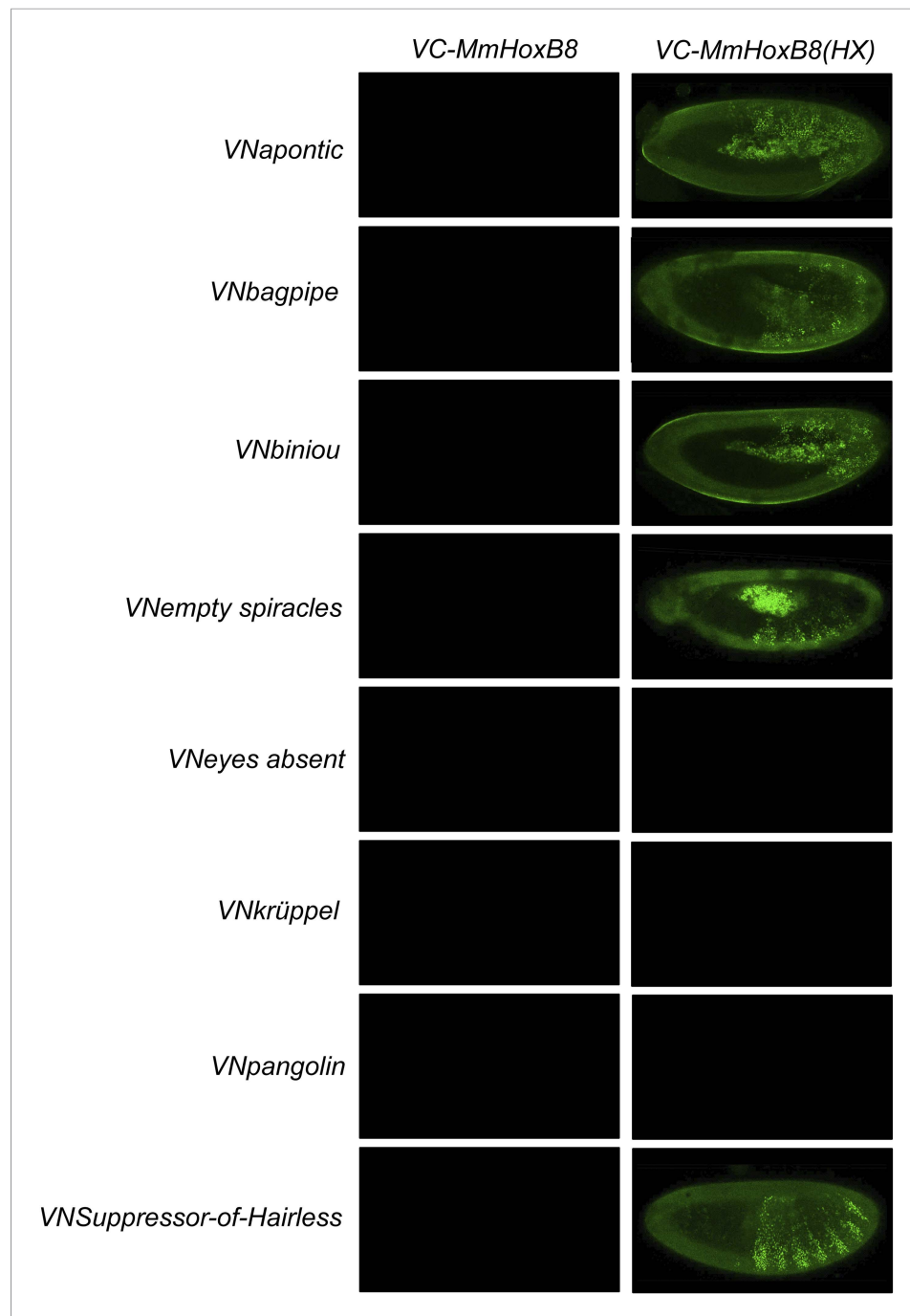
Figure 8—figure supplement 1. BiFC between *Drosophila* TFs and the mouse HoxB8 protein. Illustrative pictures are provided for each TF as indicated. No picture was taken in absence of BiFC.
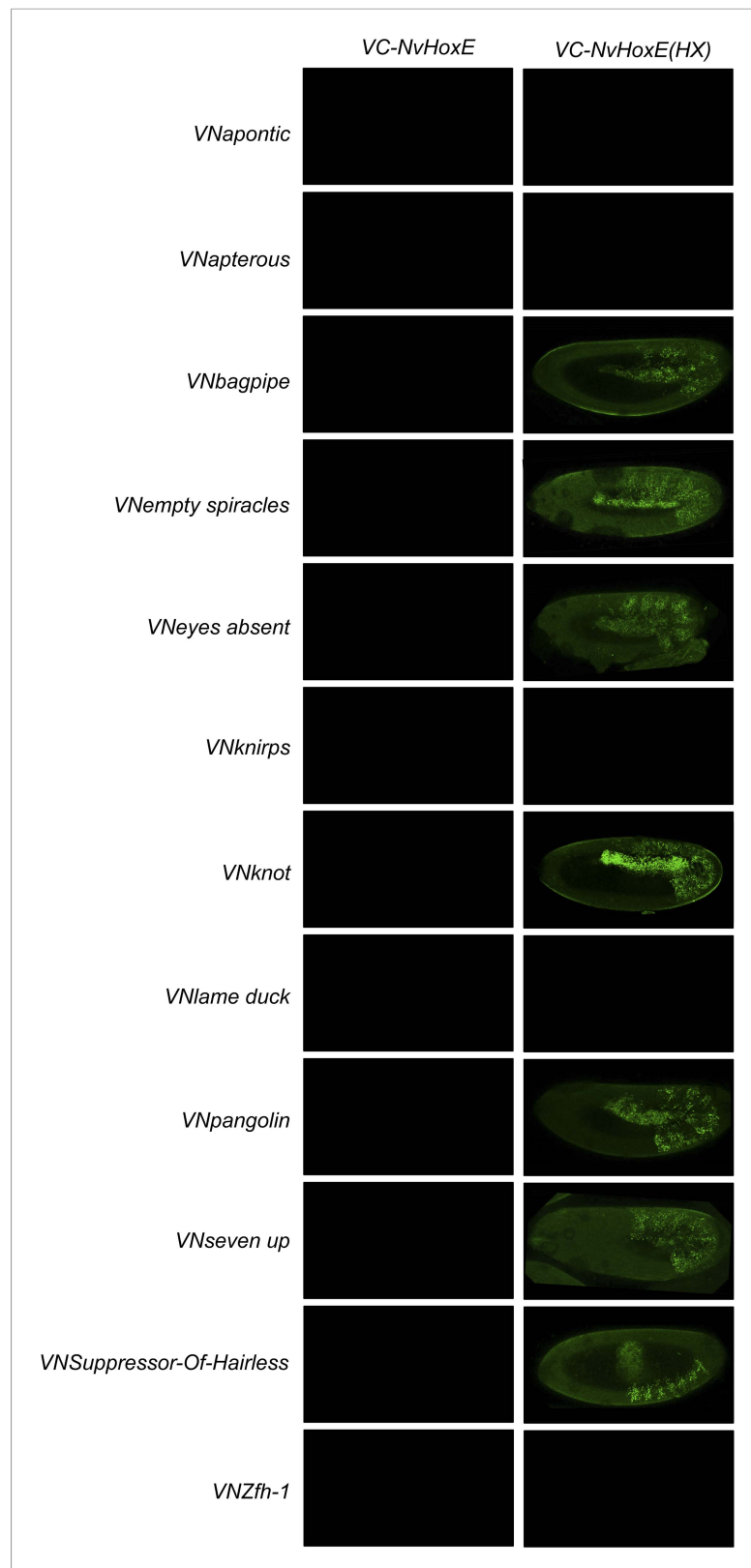DOI: 10.7554/eLife.06034.031
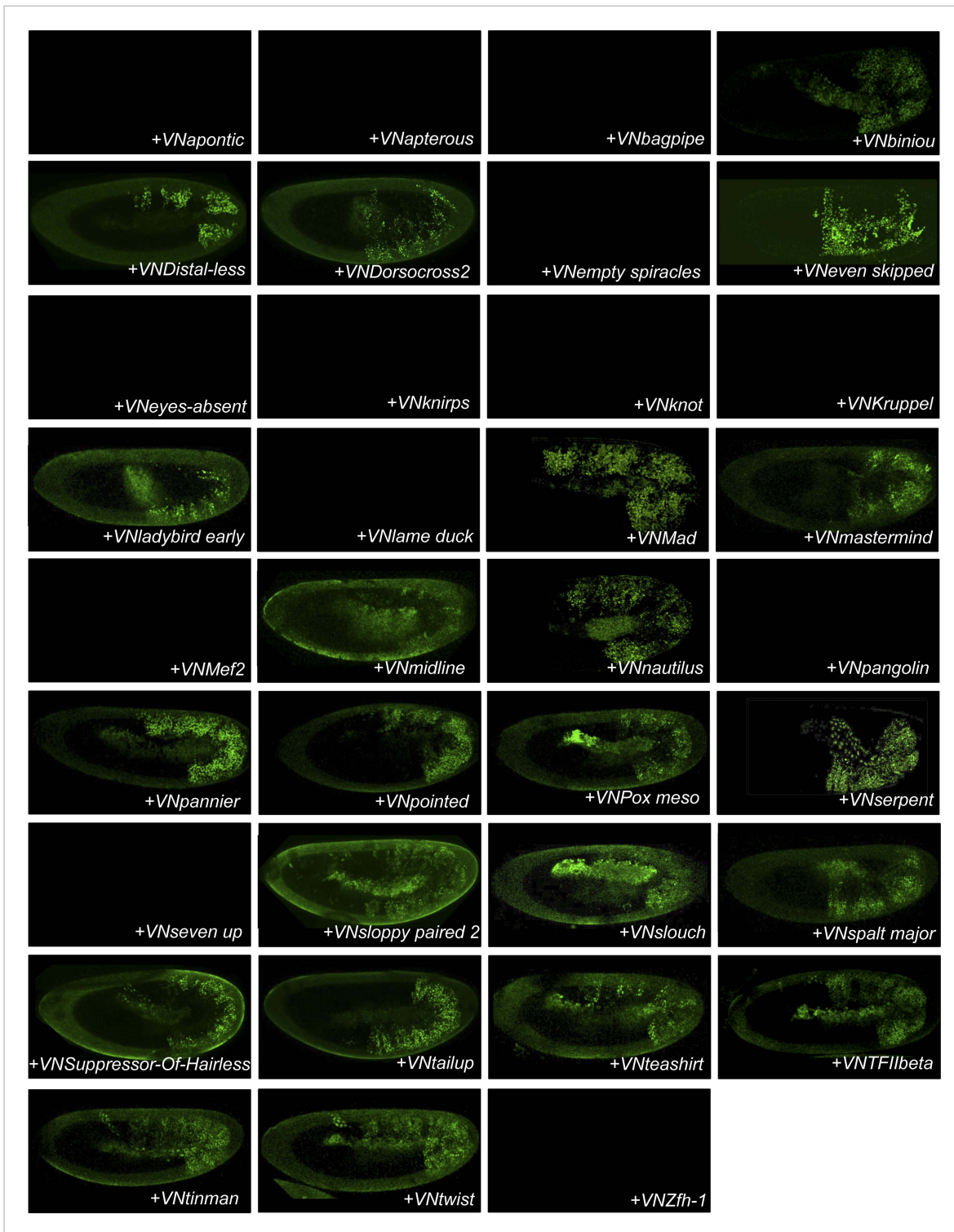
Figure 8—figure supplement 2. BiFC between *Drosophila* TFs and the *Nematostella* HoxE protein. Illustrative pictures are provided for each TF as indicated. No picture was taken in absence of BiFC.
DOI: 10.7554/eLife.06034.032

Figure 8—figure supplement 3. BiFC between *Drosophila* TFs and HX-mutated HoxB8. Illustrative pictures are provided for each TF as indicated. BiFC was performed with TFs that were negative with wild type HoxB8. The HX mutation leads to five new interactions among the eight tested TFs (as seen for Apontic, Bagpipe, Biniou, Empty spiracles and Suppressor-of-Hairless). No picture was taken in absence of BiFC.
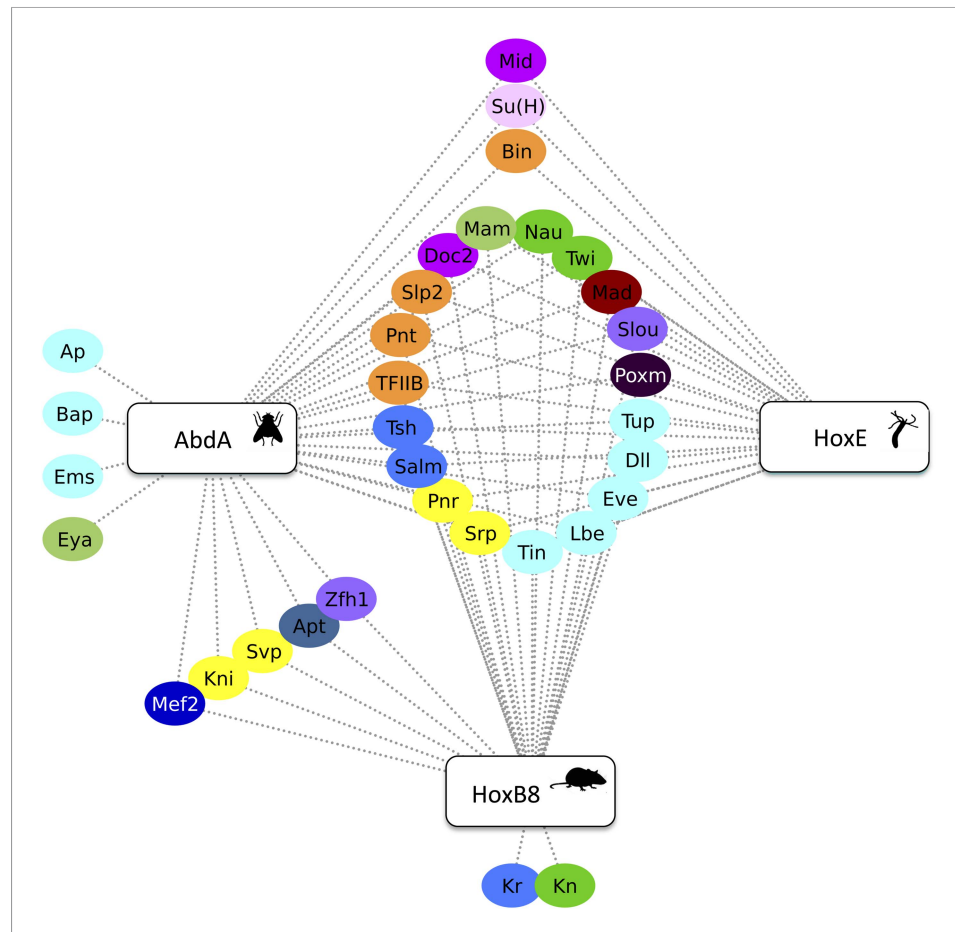DOI: 10.7554/eLife.06034.033

Figure 8—figure supplement 4. BiFC between *Drosophila* TFs and HX-mutated HoxE. Illustrative pictures are provided for each TF as indicated. BiFC was performed with TFs that were negative with wild type HoxE. The HX
Figure 8—figure supplement 4. continued on next page

Figure 8—figure supplement 5. *Drosophila* AbdA, mouse HoxB8 and *Nematostella* HoxE interact with several common TFs in vivo. Colour code and interaction representation are as in *Figure 3*.
DOI: 10.7554/eLife.06034.035
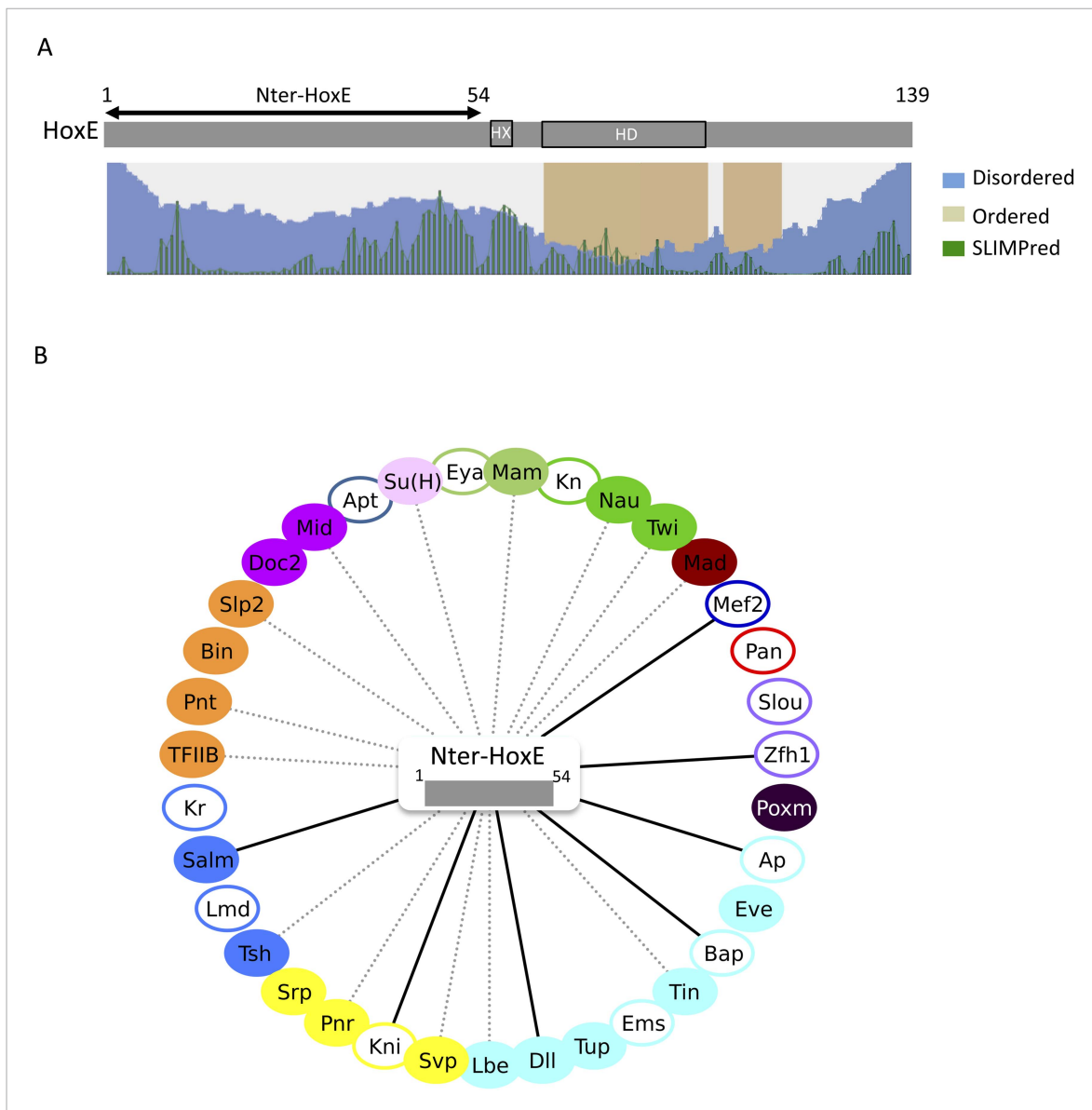
Figure 9. The intrinsically disordered region of HoxE establishes a number of interactions with *Drosophila* TFs. (**A**) Scheme of full length *Nematostella* HoxE with its predicted SLiMs (green bars), and disordered (blue waves) or ordered (brown blocks) regions. Adapted from iupred (http://iupred.enzim.hu/). The N-terminal disordered region used for BiFC is indicated (Nter-HoxE). (**B**) Interactome between Nter-HoxE and the 35 *Drosophila* TFs. Colour code and representation are as in *Figure 3*. See also *Figure 9—figure supplement 1*.
DOI: 10.7554/eLife.06034.036
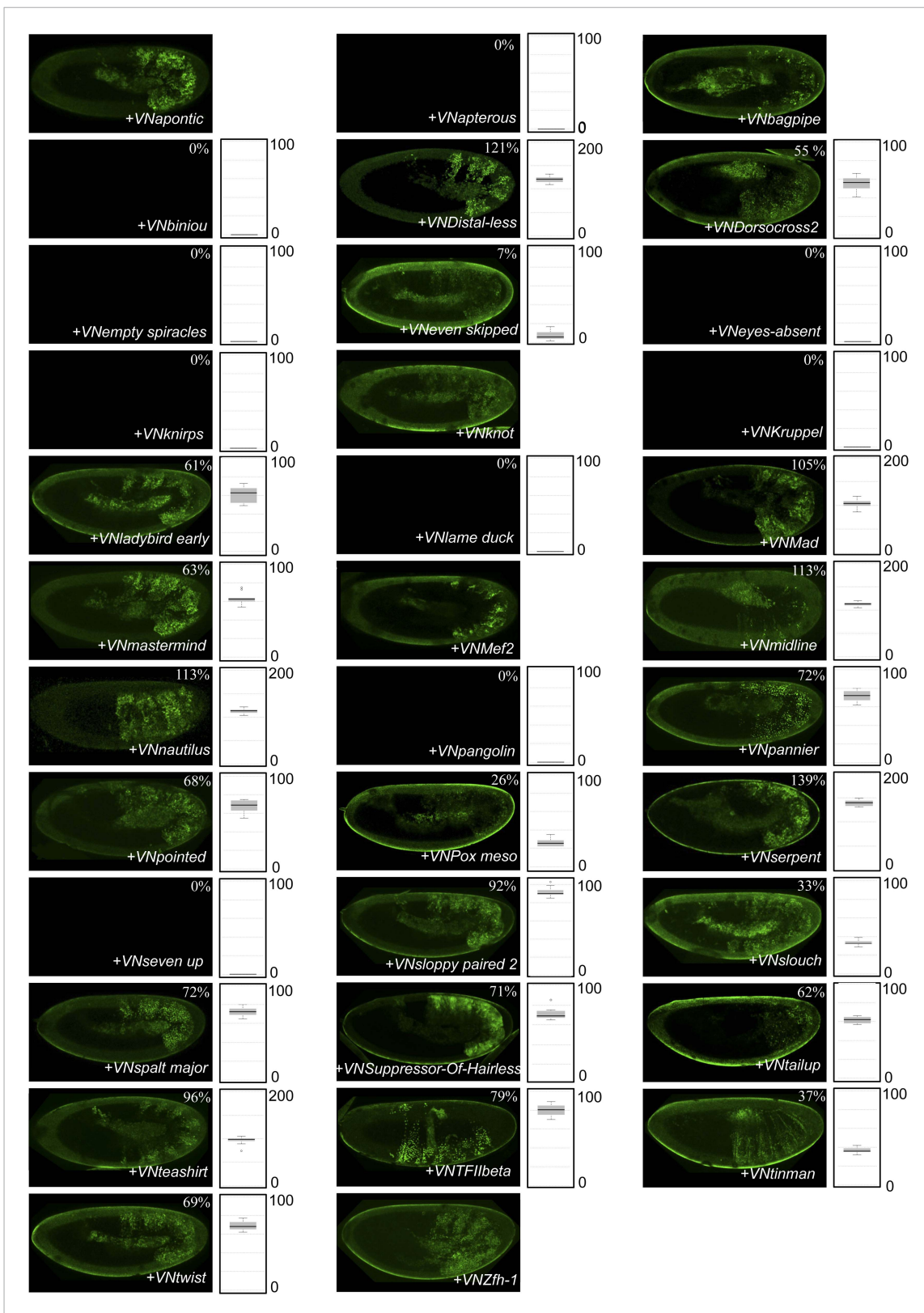
Figure 9—figure supplement 1. BiFC between *Drosophila* TFs and the N-terminal (1-54) fragment of the *Nematostella* HoxE protein. BiFC was performed with the 35 TFs in the epidermis of stage 10–12 embryos, as indicated. Quantification was performed as in **Figure 3—figure supplement 1**. No
Figure 9—figure supplement 1. continued on next page

Figure 9—figure supplement 1. Continued

statistical quantification is provided in the case of a new interaction (as seen for Apontic, Bagpipe, Knot, Mef2 and Zfh1). No picture was taken in absence of BiFC.
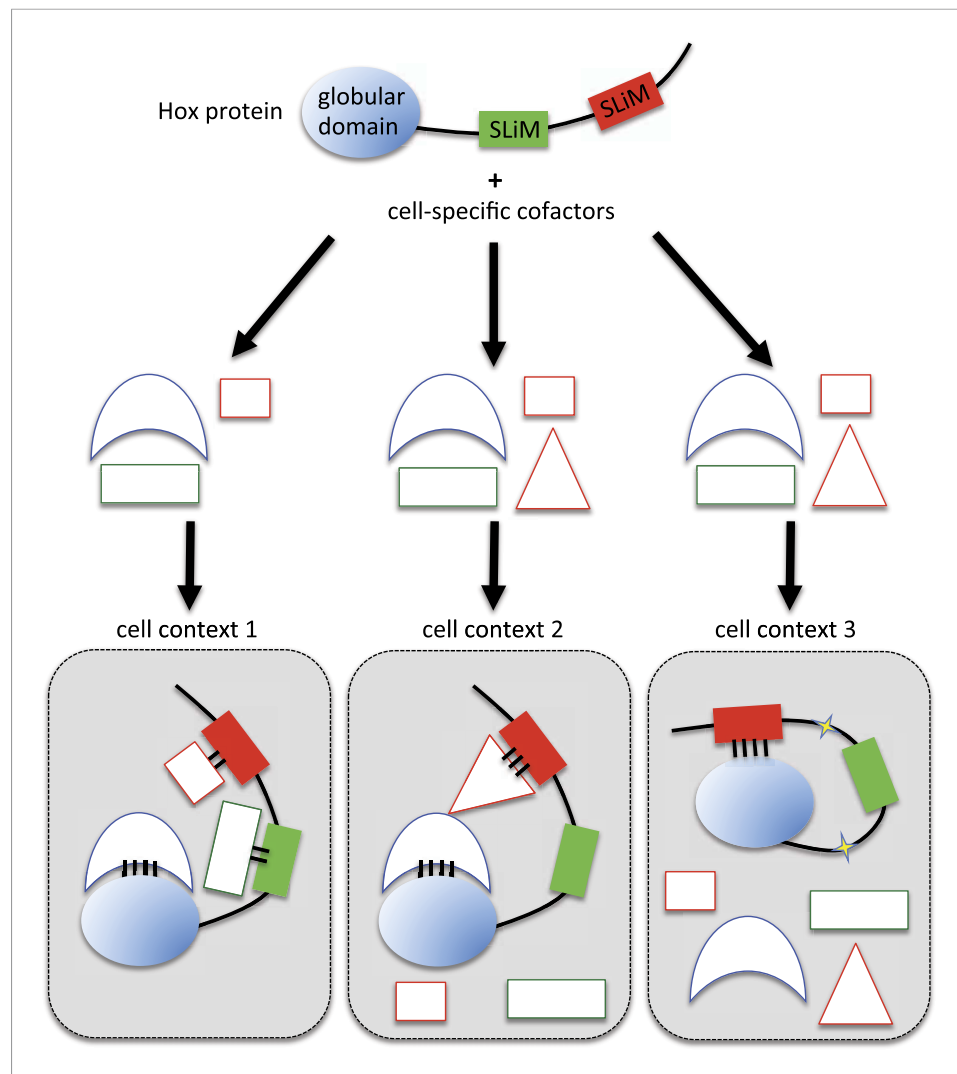
Figure 10. Molecular mechanisms underlying context-dependent activities of SLiMs in protein–protein interactions. The Hox protein is represented as containing a globular structured domain together with two different SLiMs embedded in a disordered region, as indicated. This protein will present different interaction properties with a set of cofactors that could vary depending on the cell context considered. Preferential interactions between cofactors and the protein domain and SLiMs are represented by a colour code. Black bars symbolize the various levels of interaction affinity. In the cell context 1, cofactors are recruited through specific interactions with the globular domain and the two SLiMs. In the cell context 2, there is a supplementary triangular cofactor that displays higher affinity with the red SLiM than the square cofactor. As a consequence, interaction will occur with this triangular (hiding) cofactor, which forbids the interaction with the other SLiM. In this context, the red SLiM behaves as an inhibitory interaction motif. In the cell context 3, post-translational modifications in the disordered region (yellow stars) allow the inhibitory SLiM to establish interactions in *cis* with the globular domain. These intra-molecular contacts forbid the binding of the other cofactors. The last two mechanisms illustrate how the inhibitory activity of SLiMs could help in distinguishing/specifying interactomes with an identical set of cofactors.
DOI: 10.7554/eLife.06034.038